# High Ozone Events and Attainment Demonstrations in Houston, Texas

by
Evan A. Couzo

A thesis submitted to the faculty of the University of North Carolina at Chapel Hill in partial fulfillment of the requirements for the degree of Master of Science in the Environmental Sciences and Engineering.

Chapel Hill
2010

Approved by:

William Vizuete, Advisor

Harvey Jeffries, Reader

J. Jason West, Reader

**ABSTRACT**

**EVAN A. COUZO: High Ozone Events and Attainment Demonstrations in Houston, Texas.**

**(Under the direction of William Vizuete.)**

The Houston-Galveston-Brazoria area has had multiple decades of persistent high ozone ($O_3$) values. We have analyzed ten years of ground-level measurements at 25 monitors in Houston and found that peak 1-h $O_3$ concentrations were often associated with large hourly $O_3$ increases. A non-typical $O_3$ change (NTOC) – defined here as an increase of at least 40 ppb/hr or 60 ppb/2hrs – was measured 25% of the time when concentrations recorded at a monitor exceeded the 8-h $O_3$ standard. CAMx model simulations were found to be limited in their ability to simulate NTOCs, under predicted maximum observed rates of $O_3$ increases by more than 50 ppb/hr, and had difficulty simulating spatially isolated, high $O_3$ events measured at monitors that routinely violate the 8-h $O_3$ standard. Our results suggest that this modeling system will be unable to guide the selection of effective control strategies required to meet a more stringent federal 8-h $O_3$ standard.

# Contents

# List of Tables

# List of Figures

# List of Abbreviations and Symbols

| | |
|---|---|
| $\Delta O_3$ | rate of change in ozone concentration |
| $\Delta O_{3,1h}$ | rate of change in ozone concentration over one hour period |
| $\Delta O_{3,2h}$ | rate of change in ozone concentration over two hour period |
| **AIRS** | Aerometric Information Retrieval System |
| **CAMx** | Community Air Quality Model with extensions |
| $DV_i$ | design value for monitor $i$ |
| $DVb_i$ | baseline design value for monitor $i$ |
| $DVb_{i,2006}$ | 2006 baseline design value for monitor $i$ |
| $DVb_{i,filtered}$ | filtered baseline design value for monitor $i$ |
| $DVb_{i,2006,filtered}$ | 2006 filtered baseline design value for monitor $i$ |
| $DVf_i$ | future design value for monitor $i$ |
| $DVf_{i,2018}$ | 2018 future design value for monitor $i$ |
| **EPA** | United States Environmental Protection Agency |
| HRVOC | highly reactive volatile organic compound |
| **LST** | local standard time |
| **NAAQS** | National Ambient Air Quality Standard |
| $NO_x$ | nitrogen oxides |
| NTOC | non-typical ozone change |
| $O_3$ | ozone |
| $P(O_3)$ | ozone production rate |
| **ppb** | parts per billion |
| **ppm** | parts per million |
| $RRF_i$ | relative response factor for monitor $i$ |

| | |
|---|---|
| $S_{i,B}$ | baseline simulated daily peak 8-h $O_3$ concentration at monitor $i$ |
| $S_{i,F}$ | future year simulated daily peak 8-h $O_3$ concentration at monitor $i$ |
| **SI** | special inventory |
| **SIP** | state implementation plan |
| **TCEQ** | Texas Commission on Environmental Quality |
| **TexAQS2000** | Texas 2000 Air Quality Study |
| VOC | volatile organic compound |

# Chapter 1

# Introduction

Southeast Texas has had a persistent and intractable ozone ($O_3$) pollution problem spanning the past several decades. Considerable resources in air quality modeling and measurements have been expended to better understand how high $O_3$ concentrations are formed in Houston. In 2004, a breakthrough was made in describing $O_3$ formation that led regulators to enact targeted emissions reductions. This conceptual model and subsequent emissions controls are detailed in the 2004 State Implementation Plan (SIP) mid-course review prepared by the Texas Commission on Environmental Quality (TCEQ) [1].

The TCEQ submitted to the EPA a mid-course review of their SIP for the now defunct 1-h $O_3$ National Ambient Air Quality Standard (NAAQS) in 2004. The 1-h $O_3$ SIP encompassed an eight county region around Houston and incorporated data from the Texas 2000 Air Quality Study (TexAQS-2000) field-monitoring program, an extensive ground-monitoring network, and air quality models. An analysis of the photochemical modeling data, in preparation of the SIP revision, showed that simulations consistently under predicted peak 1-h $O_3$ concentrations [2]. Very high 1-h values were measured on August 30, 2000, and, as a result, modelers focused much of their attention on this day. The analysis that ensued features prominently in the revised 1-h $O_3$ SIP. Under predictions averaged almost 60 ppb on August 30 at ground monitors

where observed 1-h $O_3$ peaks were above 150 ppb. Air samples from aircraft flying over Houston's industrial sector on that day revealed high concentrations of reactive hydrocarbons, which modeled emissions did not match [3]. It was discovered that poor model performance on August 30 could be explained by emissions adjustments alone. When emissions of highly reactive volatile organic compounds (HRVOCs) were imputed into the model, peak predicted 1-h $O_3$ concentrations were is in excess of 200 ppb, which closely matched the August 30 measurements. HRVOCs are defined as ethene, propene, 1,3-butadiene, and all butene isomers in the TCEQ's 1-h $O_3$ SIP.

Modeling results confirmed by aircraft data from the TexAQS-2000 campaign show that the highest 1-h $O_3$ peaks in Houston were often a consequence of high ozone production rates, $P(O_3)$ [4]. Calculated $P(O_3)$ for parts of Houston was two to five times greater than other major urban centers. Constrained photochemical box model calculations of $P(O_3)$ over Houston's Ship Channel were up to 80 ppb/hr [5]. These faster rates of $O_3$ production have been attributed to higher hydrocarbon reactivity, the majority of which is contributed by HRVOCs and other short-chain alkenes [3, 6, 7].

Houston's Ship Channel region contributes greatly to overall emissions of HRVOCs because it contains an unusually large density of VOC industrial point sources and one of the world's largest petrochemical manufacturing complexes. Previous studies have established that industrial VOC emissions events occur often and with notable temporal variability in Houston [8, 9, 10, 11]. At any given facility, these events are rare, but because Houston has a massive industrial network more than 1,000 events are reported each year [12]. A detailed analysis of plumes containing high $O_3$ concentrations found abnormally high concentrations of light alkenes and their oxidation products [13]. Back trajectories showed that each plume passed directly over VOC point sources surrounding the Houston Ship Channel region suggesting that these sources contributed to the observed $O_3$ production rates. Additionally, automated gas chromatograph data from

ground monitoring stations identified the Ship Channel as the most likely source of low molecular weight alkenes such as ethene and propene [14].

The research mentioned above has led to a conceptual model that explains the formation of severe $O_3$ pollution in Houston through two separable pathways. One pathway is the set of typical causes and effects that are well represented in the current 8-h NAAQS attainment methodology. The 8-h attainment methodology, however, is noticeably silent on the second pathway, which attributes localized, high rates of $O_3$ productivity to high concentrations of HRVOCs in industrial plumes. Emissions events at HRVOC point sources can lead to rapid formation of spatially isolated $O_3$ plumes, and this formation paradigm is what ultimately led the TCEQ to incorporate an EPA-approved limit on HRVOCs in their 2004 1-h $O_3$ SIP mid-course review. The HRVOC rule restricted short-term industrial emissions events to 1,200 lbs/hr and routine emissions to an annual cap. Since implementation, measured concentrations of the restricted species, as well as $O_3$ values, have declined [15, 16].

By requiring the use of a "typical" emissions inventory in photochemical models, the current attainment methodology recommended by the EPA implicitly assumes that high $O_3$ is not influenced by variable precursor emissions [17]. This assumption runs contrary to the accepted conceptual model of $O_3$ formation developed in Houston, Texas. That model, detailed in the 2004 $O_3$ SIP revision, links high $O_3$ to variable emissions of HRVOCs. Houston's unique combination and density of industrial emissions precludes the notion of an average emissions inventory. Therefore, the $O_3$ formation paradigm used to develop the 8-h NAAQS attainment methodology may not apply as readily to Houston as other non-attainment areas because Houston's airshed is impacted by stochastic HRVOC emissions.

The goal of this study is to evaluate the suitability of the 8-h NAAQS attainment process for Houston by directly comparing measurements to model simulations used for

the TCEQ's 2010 8-h $O_3$ SIP. We have developed a methodology for indentifying rapid ozone increases and determined their frequency over a ten-year period. Our earlier work showed that sudden $O_3$ concentration increases are influencing current observational attainment metrics at select monitors [18]. There, we isolated measured high $O_3$ days and found that large $\frac{d[O_3]}{dt}$ values led to the highest annual 8-h $O_3$ concentrations at several monitors. In this study, we expand our analysis and investigate whether the regulatory air quality simulations, with and without day-specific emissions, can reproduce the observed rapid $O_3$ increases. We have also compared peak 1-h and 8-h $O_3$ values simulated using the "typical" emissions inventory to peak concentrations predicted with an inventory containing day-specific emissions. The results of our analysis show that separating this phenomenon from slower ozone changes can ultimately influence the future attainment outcome for Houston. Our results suggest that the regulatory air quality models used by the TCEQ cannot accurately reproduce rapidly increasing $O_3$ concentration measurements.

# Chapter 2

# Methodology

Our study combines observational data measured at ground station monitors and photochemical air quality model predictions used by the TCEQ in the 8-h $O_3$ SIP. The TCEQ is following the EPA guidance document on attainment demonstration [17]. Our analysis used the TCEQ dataset and investigated how the 8-h attainment methodology represents extreme $O_3$ events. The relevant aspects of that process are described below followed by a description of the observed data set and model simulations.

## 2.1 Attainment Process and EPA Modeling Guidance

In 1997, the EPA set the 8-h $O_3$ NAAQS at 0.08 ppm. Compliance with the $O_3$ NAAQS is determined by comparing an observational metric to the 8-h ozone standard. This metric is called the design value ($DV_i$ for a monitor, $i$) and is a running three-year average of the annual fourth highest 8-h daily maximum $O_3$ concentrations measured at a ground monitoring station [19]. Equation 2.1 shows an example $DV_i$ calculation for a given monitor, $i$, in 2008.

$$\mathrm{DV_{i,2008}} = \frac{\mathrm{M_{i,2006}} + \mathrm{M_{i,2007}} + \mathrm{M_{i,2008}}}{3} \tag{2.1}$$

where $\mathrm{M_i}$ is the fourth highest daily peak 8-h $\mathrm{O_3}$ value observed at monitor $i$ from 2006-2008. A design value is calculated each year for all regulatory monitors in a region. If one or more $\mathrm{DV_i}$ are greater than the federal 8-h $\mathrm{O_3}$ limit, that region has failed to attain the 8-h NAAQS.

Any region that fails to meet the federal ozone standard must perform an arduous future attainment demonstration. This process, often requiring several years to complete, combines observed ground-monitoring data with baseline year and future year regulatory air quality model simulations to show that design values in the future are likely not to exceed the federal 8-h $\mathrm{O_3}$ limit. Demonstrating future attainment begins by selecting a baseline year, which provides a starting point for observations and computer model simulations, and a future attainment year by which a non-attainment region must demonstrate compliance with the NAAQS. The TCEQ selected 2006 as the baseline year and 2018 as the future year.

The future attainment demonstration is summarized in Equation 2.2 for a given monitor, $i$, using 2006 as the baseline year and 2018 as the future year.

$$\mathrm{DVf_{i,2018}} = \mathrm{RRF_i} \cdot \mathrm{DVb_{i,2006}} \tag{2.2}$$

The left-hand side of Equation 2.2 is called the future design value ($\mathrm{DVf_i}$). The $\mathrm{DVf_{i,2018}}$ is the product of an averaged observational metric ($\mathrm{DVb_i}$, baseline design value) and a quantitative measure of the simulated environmental response to proposed pollutant control strategies coupled with predicted economic growth ($\mathrm{RRF_i}$, relative response factor). A $\mathrm{DVf_{i,2018}}$ is calculated for each regulatory monitor, $i$, in a given region and must

be equal to or less than 0.08 ppm for all monitors if that region is to demonstrate future attainment of the 1997 8-h $O_3$ NAAQS.

$DVb_i$ and $RRF_i$ are also calculated for each regulatory monitor, $i$. The $DVb_i$ is an average of three consecutive $DV_i$ as shown in Equation 2.3.

$$DVb_{i,2006} = \frac{DV_{i,2006} + DV_{i,2007} + DV_{i,2008}}{3} \tag{2.3}$$

In this example calculation, five years of measured data are weighted most heavily towards 2006. This is a desired effect as 2006 is the baseline year for the future attainment demonstration and serves as the anchor point for model predictions.

The $RRF_i$ is the ratio of model-predicted $O_3$ concentrations in the future to model-predicted baseline $O_3$ concentrations at a monitor, $i$. A small $RRF_i$ indicates a large percent reduction of $O_3$ concentrations and, hence, a lower $DVf_i$ . Equation 2.4 shows how $RRF_i$ is calculated for a monitor, $i$.

$$RRF_i = \frac{\overline{S_{i,F}}}{\overline{S_{i,B}}} \tag{2.4}$$

where $\overline{S_{i,F}}$ and $\overline{S_{i,B}}$ are mean future year and baseline predicted maximum 8-h $O_3$, respectively. The mean predictions are defined in Equations 2.5 and 2.6 for a monitor, $i$.

$$\overline{S_{i,F}} = \frac{\sum_{d=1}^{D} S_{i,F,d}}{D} \tag{2.5}$$

$$\overline{S_{i,B}} = \frac{\sum_{d=1}^{D} S_{i,B,d}}{D} \tag{2.6}$$

where $S_i$ is the simulated daily peak 8-h concentration at monitor $i$, $D$ is the number of days used in the calculation, $F$ is the future year, and $B$ is the baseline. Not all

simulated days are used to calculate the $RRF_i$. Only after meeting EPA recommended qualifications are simulated days used in Equation 2.6; the exact same days are always used in Equation 2.5. Details on day selection can be found in the EPA guidance document.

## 2.2 Observational Data Set

Observed data were obtained from the TCEQ website, which provides hourly averaged measurement data [20]. Twenty-five monitoring stations were used in this study, and they are listed in Table 2.1 with their official names, 4-letter abbreviation, TCEQ identification number, and Aerometric Information Retrieval System (AIRS) number; these are the same monitors used in the TCEQ's 8-h SIP. Monitor locations are shown in Figure 2.1. The four highest 8-h $O_3$ days for each year at each monitor were identified for 2000 through 2009, and a subset of those days (2004-2008) was used to calculate a $DVb_i$ for each location. The results of the $DVb_i$ calculations are listed in Table 4.1.

## 2.3 Air Quality Model Data Set

The TCEQ used the Community Air Quality Model with extensions (CAMx) version 4.53 model [21] to create 2005 and 2006 baseline conditions and projected 2018 conditions for six modeling episodes. Table 2.2 provides a summary of each episode with the naming conventions used by the TCEQ. Detailed documentation concerning the development of the inputs for these episodes can be found on the TCEQ website [22]. In total, there are 120 modeling days in the 2005 and 2006 episodes. To support a multi-species model performance assessment, the TCEQ generated a base case inventory for the six episodes. This included the development of an hourly special inventory (SI) that was based on reports from 125 facilities in the region for the period of August

Table 2.1: List of ground monitoring stations and their identifying information. The TCEQ uses CAMS (continuous ambient monitoring stations) numbers; the EPA uses AIRS (aerometric information retrieval system) numbers.

| Monitor Name | Abbreviation | CAMS No. | AIRS No. |
|---|---|---|---|
| Bayland Park | BAYP | 53 | 48-201-0055 |
| Clinton | CLIN | 403 | 48-201-1035 |
| Conroe Relocated | CNR2 | 78 | 48-339-0078 |
| Danciger | DNCG | 618 | 48-039-0618 |
| Deer Park | DRPK | 35 | 48-201-1039 |
| Galveston | GALC | 34 | 48-167-0014 |
| HRM-3 Haden Road | H03H | 603 | 48-201-0803 |
| Aldine | HALC | 8 | 48-201-0024 |
| Channelview | HCHV | 15 | 48-201-0026 |
| Croquet | HCQA | 409 | 48-201-0051 |
| Lang | HLAA | 408 | 48-201-0047 |
| Northwest Harris County | HNWA | 26 | 48-201-0029 |
| Houston East | HOEA | 1 | 48-201-1034 |
| Houston Regional Office | HROC | 81 | 48-201-0070 |
| Monroe | HSMA | 406 | 48-201-0062 |
| Texas Avenue | HTCA | 411 | 48-201-0075 |
| North Wayside | HWAA | 405 | 48-201-0046 |
| Lake Jackson | LKJK | 1016 | 48-039-1016 |
| Lynchburg Ferry | LYNF | 1015 | 48-201-1015 |
| Manvel Croix Park | MACP | 84 | 48-039-1004 |
| Mustang Bayou | MSTG | 619 | 48-039-0619 |
| Seabrook Friendship Park | SBFP | 45 | 48-201-1050 |
| Westhollow | SHWH | 410 | 48-201-0066 |
| Texas City | TXCT | 620 | 48-167-0056 |
| Wallisville | WALV | 617 | 48-201-0617 |

15, 2006 to September 15, 2006. These dates coincide with a second field campaign, during which hourly emissions rates were collected from over 1,200 VOC emissions point sources. A goal of integrating the SI into photochemical modeling is to reproduce the stochastic emissions inventory in Houston.

For the attainment demonstration, the 2006 baseline and 2018 future year inventories were constructed consistent with EPA inventory guidance. That is, the emissions files used for the model evaluation were changed to comport with EPA's "typical" emissions criteria. This was accomplished by dropping day-specific emissions data – such as the hourly SI – and reverting to ozone season averaged daily emissions at electric

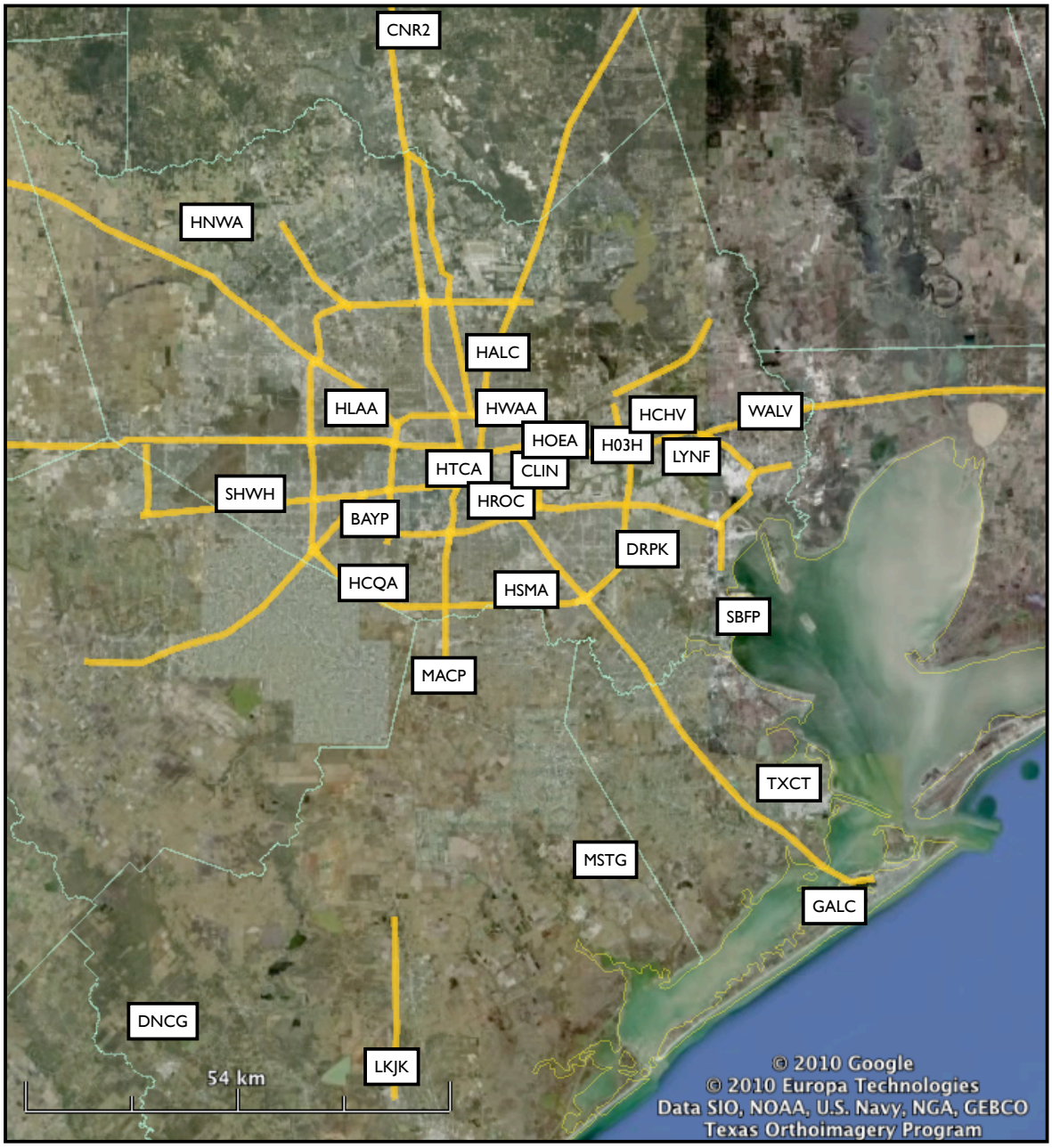


Figure 2.1: Location of the surface monitors used in this study.

generating units and VOC point sources. In addition to being used in the attainment demonstration, the baseline emissions inventory was the basis for the 2018 emissions inventory. The emissions inventory for 2018 includes all existing emissions controls, projected growth of emissions, and proposed emissions controls. Specific differences

between the emissions inventories are described in the 2010 8-h SIP, but a summary can be found in Table 2.3. It is important to note that the 2005 and 2006 model simulations used in the $RRF_i$ calculations retained their date-specific meteorology.

The TCEQ used a regional 36-km domain and 12-km Eastern Texas subdomain to provide boundary conditions for a 4-km Houston Galveston Brazoria/Beaumont Port Arthur subdomain. A finely resolved 2-km Houston Galveston subdomain was also developed, and all model files used in this study are from this 2-km subdomain. Figure 2.2 shows the nested domain structure. Detailed horizontal and vertical domain documentation can be found on the TCEQ website [23]. Meteorological inputs were resolved at the 4-km level. The TCEQ utilized the flexi-nesting option of CAMx to interpolate 2-km meteorological fields.

One-hour $O_3$ concentrations were extracted from each ground layer grid cell, and $RRF_i$ were calculated for each monitor. Table 4.1 contains the results of these calculations. When calculating the maximum daily 8-h average $O_3$ concentration for a monitor, the EPA allows the use of any grid cell "near" the monitor in anticipation of the uncertainty involved in simulating exactly high $O_3$ locations [17]. The TCEQ used 7x7 grid cell arrays centered on each monitor location from which $S_{i,B}$ and $S_{i,F}$ were chosen. The grid cell selected in the baseline simulation does not have to be the same grid cell used in

Table 2.2: Regulatory air quality modeling episodes created by the TCEQ to support their 2010 8-h $O_3$ SIP. Included are the simulation periods and the naming conventions used by the TCEQ for their emissions inventories and meteorological data files.

| Developer | Model Software | Simulation Period | Emission Inventory | | | | Met. File Name | Chemical Mechanism |
|---|---|---|---|---|---|---|---|---|
| | | | Base Case | Base Line | | Future | | |
| | | | Name | Name | Year | Name | | |
| TCEQ | CAMx v4.53 | 2005-05-19 to 2005-06-03 | reg10 | reg2 | 2006 | cs04 | eta_dbemis_fddats_newuhsst_newutcsrlulc_grell.v45 | CB05 |
| | | 2005-06-17 to 2005-06-30 | | | | | | |
| | | 2005-07-26 to 2005-08-08 | | | | | | |
| | | 2006-05-31 to 2006-06-15 | | | | | | |
| | | 2006-08-13 to 2006-09-15 | reg10si | | | | | |
| | | 2006-09-16 to 2006-10-11 | reg10 | | | | | |

TCEQ=Texas Commission on Environmental Quality

CB05=Carbon Bond Mechanism version 5

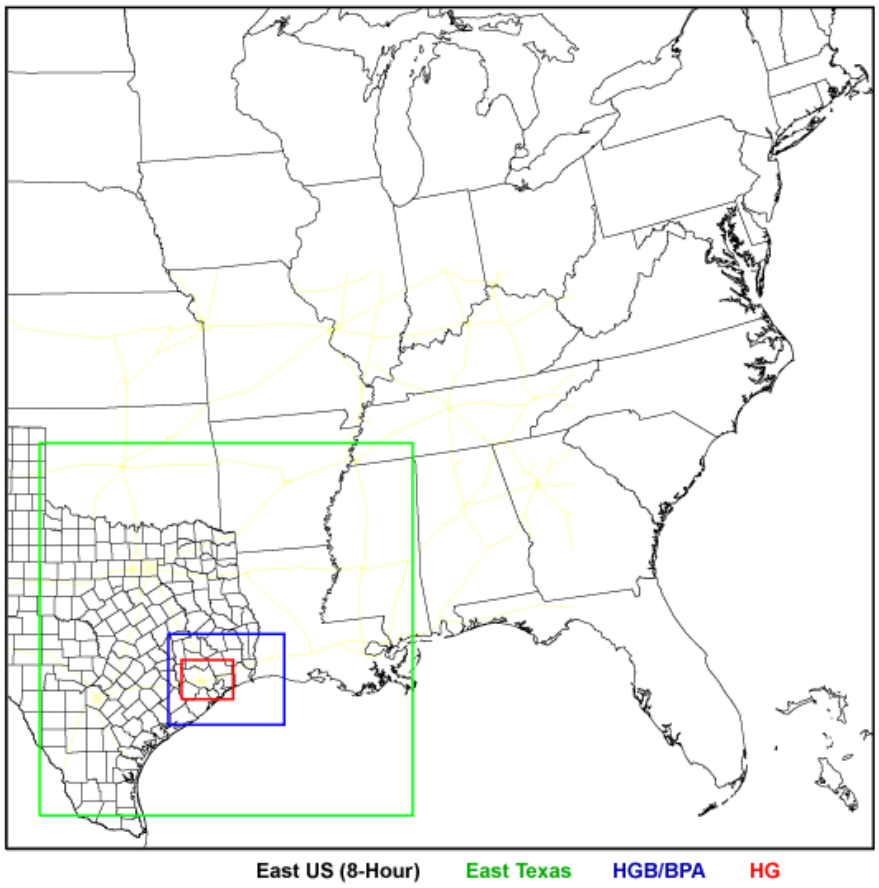


Figure 2.2: Nested CAMx domain structure. East US is 36-km; East Texas is 12-km; HGB/BPA is 4-km; and HG is 2-km. All modeling data used in this study was extracted from the HG 2-km domain.

the future year simulation, and, in fact, it often changes location [24]. We followed this approach of selecting from the monitor-centered 7x7 array each grid cell with the maximum predicted 8-h $O_3$ concentration. Unless otherwise specified, simulated daily maxima "at a monitor" refers to the grid cell with the greatest calculated 8-h average value and not necessarily the exact grid cell in which the monitor is located.

Table 2.3: Emissions inventories for the eight county non-attainment area. Shows the 2006 base case inventory in tons per day. Values for the baseline and future year inventories are given relative to the base case. Blue values denote increases relative to the base case; red values denote decreases relative to the base case.

| Source Category | Eight County Area Emissions Inventories | | | | | | | | |
|---|---|---|---|---|---|---|---|---|---|
| | 2006 base case | | | base case to 2006 base line Gains and Losses | | | base line to 2018 future Gains and Losses | | |
| | *CO* | *NOX* | *VOC* | *CO* | *NOX* | *VOC* | *CO* | *NOX* | *VOC* |
| On-road (link) - diesel | 7.7 | 32.9 | 1.7 | 0.0 | 0.0 | 0.0 | (3.4) | (16.1) | 1.1 |
| On-road (link) - gasoline | 1,015.0 | 151.6 | 80.3 | 0.0 | 0.0 | 0.0 | (364.5) | (122.2) | (42.7) |
| On-road (idling) | 0.5 | 2.4 | 0.1 | 0.0 | 0.0 | 0.0 | (0.4) | (1.9) | 0.0 |
| **On-Road, total** | **1,023.2** | **186.8** | **82.0** | **0.0** | **0.0** | **0.0** | **(368.3)** | **(140.2)** | **(41.6)** |
| Point EGU | 23.3 | 21.5 | 1.9 | (0.6) | 1.9 | 0.1 | 20.7 | 7.7 | 2.3 |
| Area EGU | | | | | | | | | |
| **EGU, total** | **23.3** | **21.5** | **1.9** | **(0.6)** | **1.9** | **0.1** | **20.7** | **7.7** | **2.3** |
| Point non-EGU | 35.7 | 52.9 | 3.0 | 12.0 | 57.0 | 2.9 | (7.2) | (64.4) | (0.8) |
| Area non-EGU | 5.6 | 9.0 | 0.4 | 0.0 | 0.0 | 0.0 | (0.2) | (0.2) | (0.0) |
| **non-EGU, total** | **41.4** | **61.8** | **3.4** | **12.0** | **57.0** | **2.9** | **(7.3)** | **(64.6)** | **(0.8)** |
| Point petrochemical/O&G | 53.1 | 50.2 | 119.4 | 37.9 | 12.0 | 15.7 | (18.6) | 0.9 | 114.6 |
| Point SI petrochemical/O&G | | 26.7 | 25.8 | | (26.7) | (25.8) | | 0.0 | 0.0 |
| Point SI other | | 24.1 | 3.4 | | (24.1) | (3.4) | | 0.0 | 0.0 |
| Point PSCF (petrochem) | | | 32.1 | | | 0.0 | | | (6.3) |
| Point Landing Losses (petrochem) | | | 4.4 | | | 3.7 | | | 0.0 |
| Area petrochemical/O&G | 22.5 | 19.9 | 252.9 | 0.0 | 0.0 | 0.0 | 0.0 | (0.0) | 0.3 |
| **Petrochemical/O&G, total** | **75.7** | **120.8** | **437.9** | **37.9** | **(38.8)** | **(9.7)** | **(18.6)** | **0.8** | **108.6** |
| Point wildfires | 3.2 | 0.0 | 0.2 | (3.2) | (0.0) | (0.2) | 0.0 | 0.0 | 0.0 |
| Area fires | 1.4 | | | 0.0 | | | 0.0 | | |
| **Fires, total** | **4.5** | **0.0** | **0.2** | **(3.2)** | **(0.0)** | **(0.2)** | **0.0** | **0.0** | **0.0** |
| Point ships | 5.2 | 34.2 | 0.2 | 0.0 | 0.0 | 0.0 | 0.9 | 6.3 | 0.9 |
| Area off-road (TX) | 23.3 | 38.4 | 3.4 | 0.0 | 0.0 | 0.0 | (14.9) | (2.3) | (1.0) |
| Area off-road (other) | 28.9 | 10.3 | 17.6 | 0.0 | 0.0 | 0.0 | (4.5) | 1.9 | (14.9) |
| Area non-road | 635.6 | 70.7 | 63.5 | 0.0 | 0.0 | 0.0 | 196.5 | (30.9) | (12.4) |
| **Non-Road, total** | **692.9** | **153.5** | **84.8** | **0.0** | **0.0** | **0.0** | **178.0** | **(25.0)** | **(27.4)** |
| **Point unclassfied** | **9.5** | **3.8** | **16.1** | **0.0** | **0.1** | **5.4** | **2.0** | **1.4** | **5.1** |
| **Area unclassified** | **72.8** | **2.4** | **119.7** | **0.0** | **0.0** | **0.0** | **(2.6)** | **(0.0)** | **(2.9)** |
| Area, total | 102.4 | 31.3 | 373.0 | 0.0 | 0.0 | 0.0 | (2.7) | (0.3) | (2.5) |
| Non-road, total | 692.9 | 153.5 | 84.8 | 0.0 | 0.0 | 0.0 | 178.0 | (25.0) | (27.4) |
| On-road, total | 1,023.2 | 186.8 | 82.0 | 0.0 | 0.0 | 0.0 | (368.3) | (140.2) | (41.6) |
| Point, total | 130.0 | 213.4 | 206.4 | 46.2 | 20.1 | (1.6) | (2.2) | (48.2) | 115.8 |
| **Total** | **1,948.5** | **585.0** | **746.3** | **46.2** | **20.1** | **(1.6)** | **(195.3)** | **(213.7)** | **44.3** |

# Chapter 3

# Results

Upon examining the observational records of ground monitors, it became clear that two types of ozone evolution are present in Houston. Frequently, 1-h $O_3$ time series exhibit "typical" increases of 10-30 ppb/hr. This is consistent with most calculated $P(O_3)$ rates in Houston and other urban centers [4]. Occasionally, however, ground monitoring stations observe what we call non-typical ozone changes (NTOCs) that are characterized by rapid concentration increases. It has been observed that some of the NTOCs are accompanied by HRVOCs originating from industrial sources. Figure 3.1 shows 1-h $O_3$ time series plots for the HALC monitor on two different days in 2003. The time series shows the hourly averaged $O_3$ concentration in red and hourly resultant wind vectors in blue. The green line represents the peak 8-h $O_3$ concentration, the 8-h window that was used, and a black arrow shows the 8-h resultant wind vector. The left-hand plot is characteristic of typical ozone pollution. Though the peak 8-h value is well above the federal standard, maximum concentration increases are little more than 20 ppb/hr. The right-hand plot, dominated by a 1-h $O_3$ increase of 102 ppb, illustrates a NTOC . As a result of the rapid increase, the peak 1-h value in the right-hand plot is over 100 ppb greater than in the other plot. Peak 8-h $O_3$ concentrations between the two plots are comparable, though, indicating that there are multiple $O_3$ formation pathways that can lead to violations of the 8-h $O_3$ NAAQS. The non-typical $O_3$ change

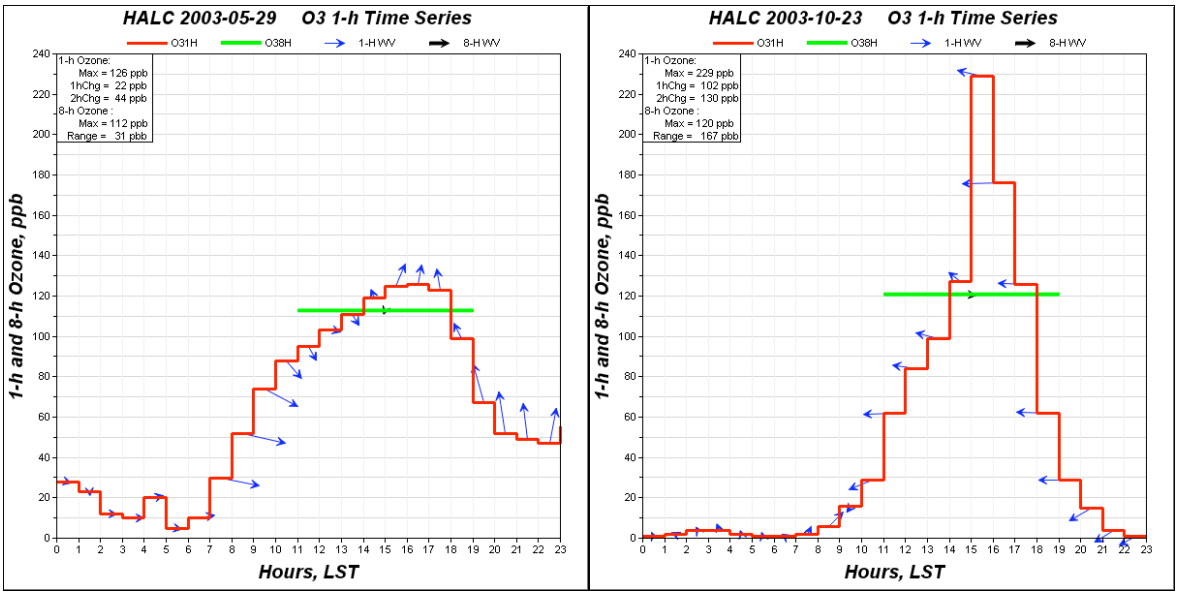


Figure 3.1: $O_3$ time series plots from measurements. Hourly averaged $O_3$ concentrations are shown in red and hourly resultant wind vectors in blue. The green line represents the peak 8-h $O_3$ concentration, the 8-h window that was used, and a black arrow shows the 8-h resultant wind vector. The plot on the left is exhibits only typical $O_3$ changes, and the plot on the right is characteristic of NTOC behavior.

measured on October 23, 2003, is thought to be related to emissions variability because high concentrations of HRVOCs were observed at nearby automated gas chromatograph stations at the start of the high $O_3$ event.

## 3.1 Observed Non-Typical Ozone Changes

Two criteria were used to identify and classify NTOC days at a monitor in the observational data: (1) any change in $O_3$ from hour-to-hour ($\Delta O_{3,1h}$) equal to or greater than 40 ppb, and (2) any change in $O_3$ over two hours ($\Delta O_{3,2h}$) equal to or greater than 60 ppb. The TCEQ and others have used criterion 1 to identify high $O_3$ plumes likely caused by an emissions event [1, 25]. Criterion 2 recognizes the fact that the HRVOC rule implemented by the TCEQ has successfully decreased the magnitudes of HRVOC

emissions, so 1-h $O_3$ increases may be less than 40 ppb per hour.

The NTOC criteria were applied to all measurement data. Results of this analysis revealed that there were 1,095 monitor-days that met either NTOC criterion. Figure 3.2 shows the distribution of measured $\Delta O_{3,1h}$ and subsequent 1-h concentrations for 2000-2009 (top left) and 2004-2008 (top right). The red horizontal lines mark hourly

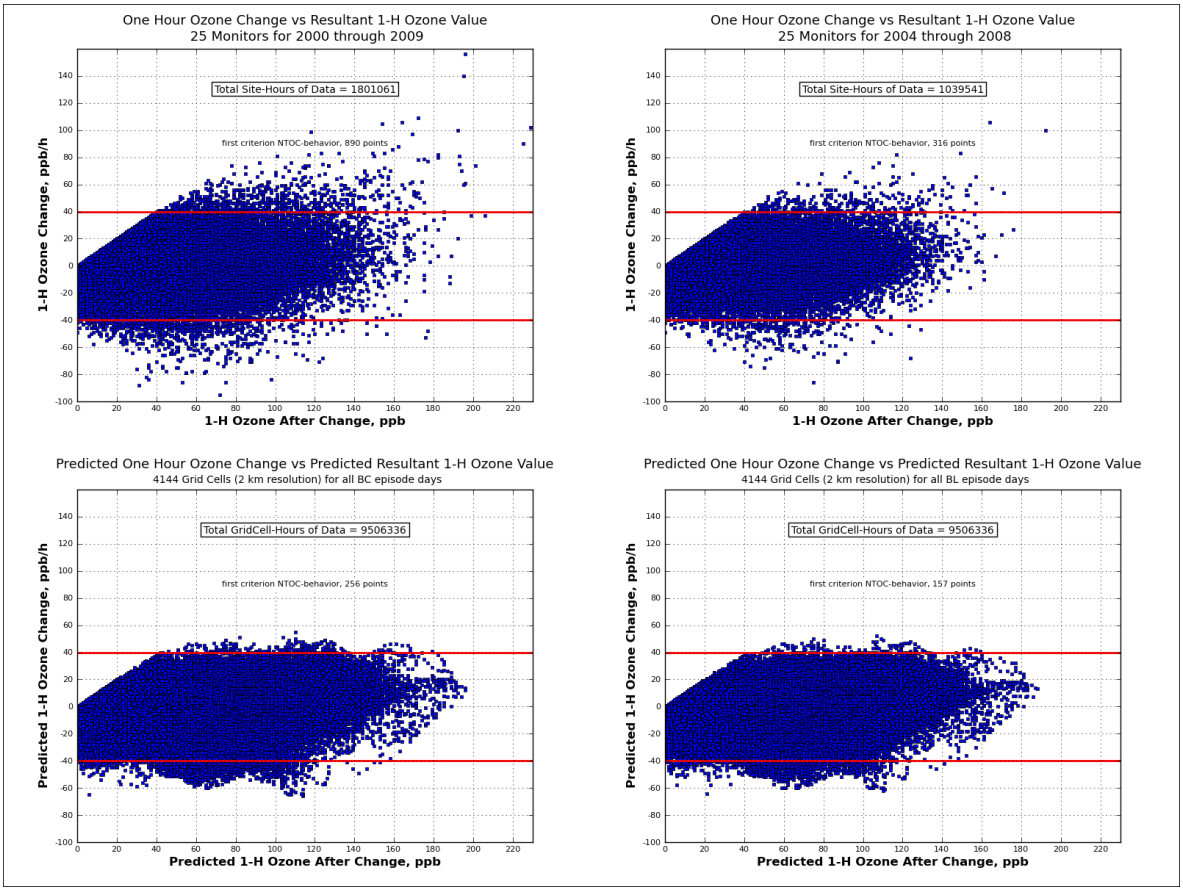


Figure 3.2: Scatter plots comparing hourly $O_3$ changes to the resulting 1-h $O_3$ concentration after each change. The plot on the top left shows all measurements from 2000-2009. The plot on the top right shows measurements from the 2004-2008 attainment period. The bottom left and bottom right plots show base case and baseline predictions for all episode days, respectively. Only the base case simulation (bottom left) uses the SI; the baseline simulation has day-specific emissions removed. The horizontal red lines mark one-hour $O_3$ changes of 40 ppb/hr. Any hourly increase above the top red line is considered a NTOC.

concentration changes of ± 40 ppb/hr, thus all data points above the top red line meet the first NTOC criterion. The five-year data subset was used determine if NTOCs occurred during the attainment period used in the TCEQ's 2010 $O_3$ SIP. While it is apparent that the most extreme $\Delta O_{3,1h}$ and 1-h concentrations occurred before 2004, NTOCs were measured during the attainment window. From 2004-2008, a wide range of $\Delta O_{3,1h}$ was measured with two data points reaching 100 ppb/hr. Figure 3.2 illustrates that both typical and non-typical $\Delta O_3$ can lead to high 1-h values, but it is noteworthy that the greatest measured 1-h concentration was the result of a large hourly increase.

NTOC days are generally subject to higher 1-h and 8-h peak concentrations than

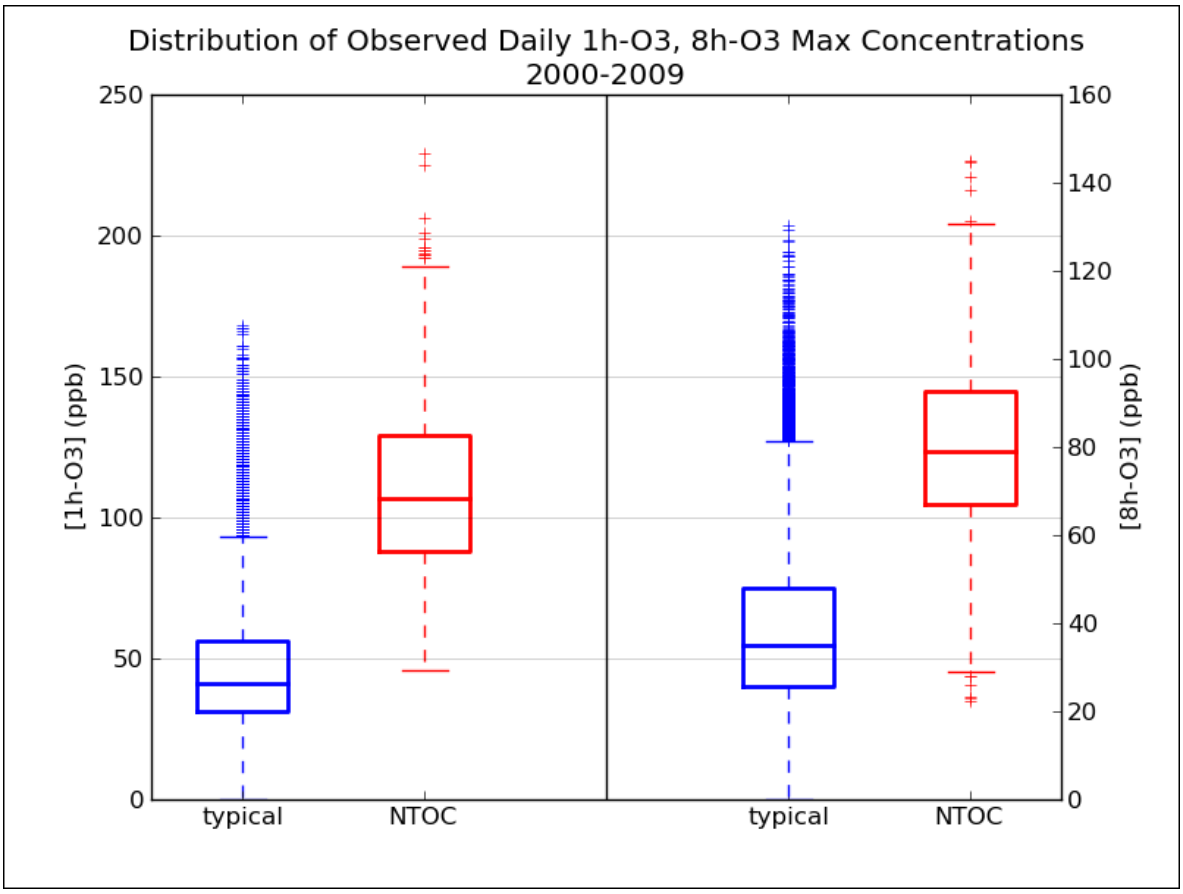


Figure 3.3: Distributions of 1-h and 8-h daily peak $O_3$ concentrations for typical and NTOC days for all measurements from 2000-2009. The plot on the left gives 1-h maxima, and the plot on the right shows 8-h maxima.

typical days. In Figure 3.3, we have separated NTOC days from typical days for all measurements during 2000-2009 and plotted the distributions of measured 1-hr and 8-h daily maxima. NTOC days have higher peak values. The greatest 1-h peak measured on a NTOC day was 229 ppb; 1-h peaks on typical days never reached 170 ppb. Figure 3.3 also shows that NTOC days are more likely to coincide with an exceedance of the 0.08 ppm federal standard. Forty percent of NTOC days exceeded the 8-h NAAQS compared to less than 5% of all typical ozone change days.

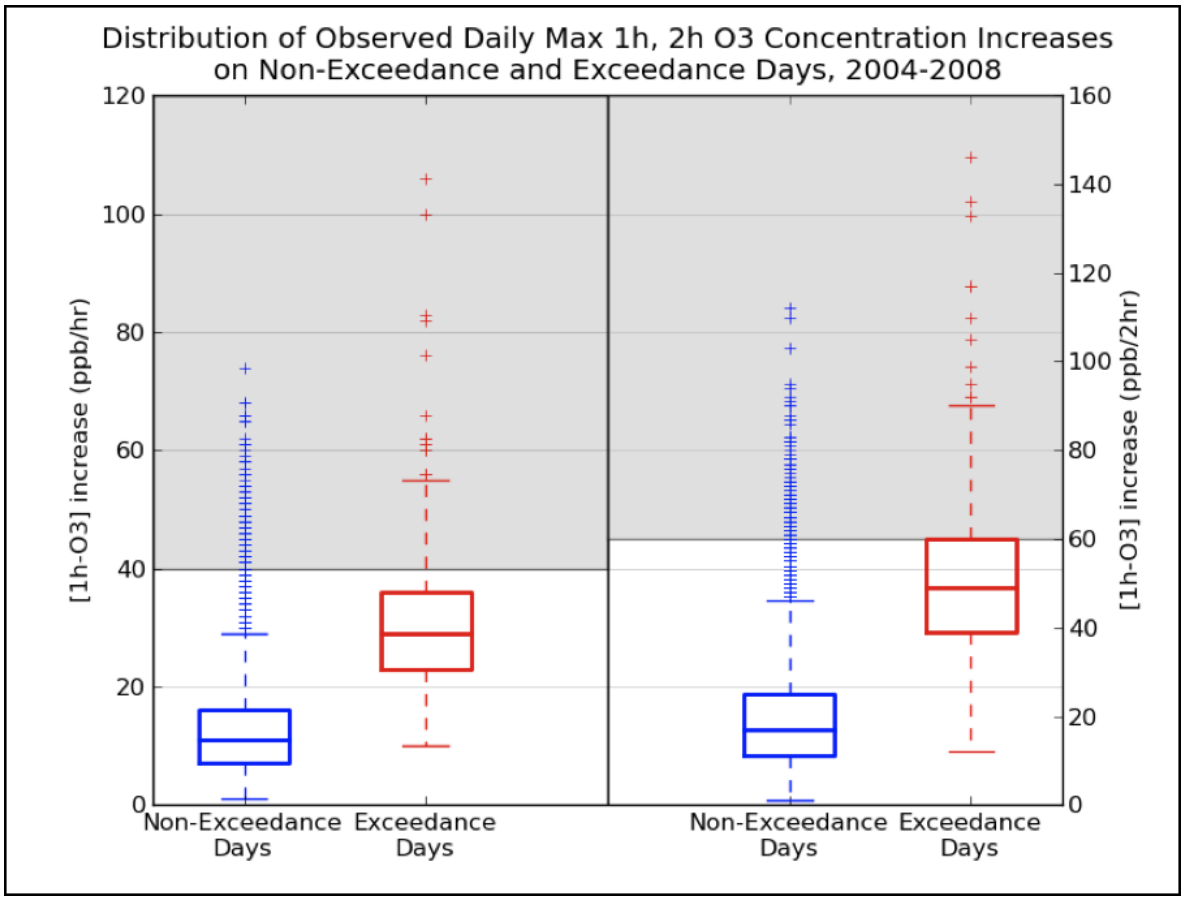


Figure 3.4: Distributions of daily maximum one-hour and two-hour $O_3$ concentration increases for non-exceedance and exceedance days for all measurements from 2004-2008. Exceedance days have a peak 8-h $O_3$ concentration of 85 ppb or above. The plot on the left gives maximum hourly increases, and the plot on the right shows maximum two-hour increases. The gray shaded regions mark the NTOC criteria, i.e. at least 40 ppb/hr and 60 ppb/2hrs.

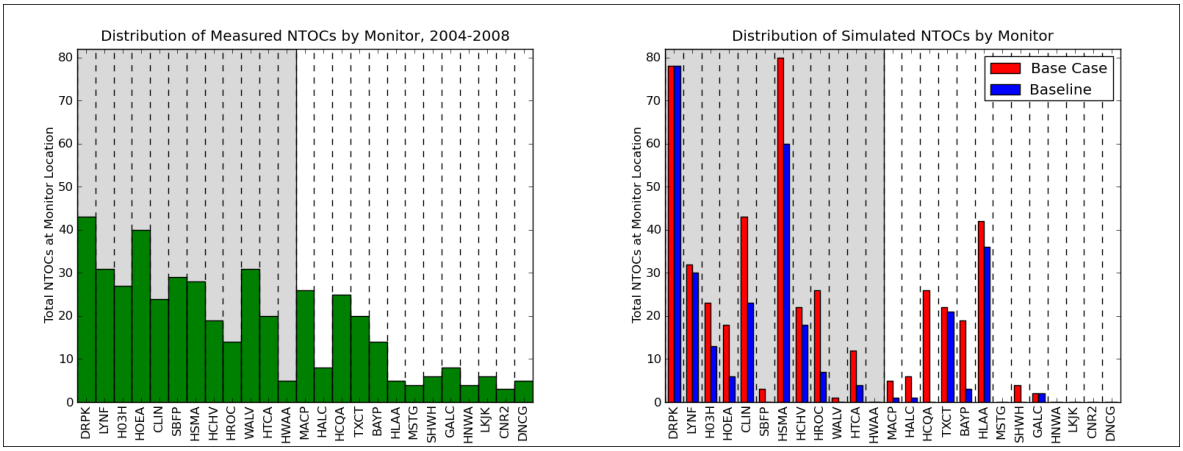


Figure 3.5: Spatial distribution of NTOCs measured and simulated at each monitor. Bar heights indicate the number of NTOCs measured and simulated at a particular monitoring site. Monitors are ordered according to increasing radial distance from the DRPK monitor, which is near the Ship Channel. The 12 monitors within the shaded region are within 20 km of the DRPK monitor.

Daily peak 8-h concentrations were calculated and paired with maximum $\Delta O_{3,1h}$ and $\Delta O_{3,2h}$ for each day of measurements during the 2004-2008 attainment period. If the 8-h peak was greater than 0.08 ppm, it was classified as an exceedance day for that monitor; exceedance days at all monitors were aggregated. All 8-h maxima less than or equal to the NAAQS were similarly gathered. Figure 3.4 plots the distribution of $\Delta O_{3,1h}$ and $\Delta O_{3,2h}$ for the two aggregate groups, exceedance and non-exceedance. Ozone exceedances were more likely on days with greater hourly concentration increases. Almost one in five exceedances coincided with a $\Delta O_{3,1h}$ greater than 40 ppb, and one in four occurred when the $\Delta O_{3,2h}$ was measured to be at least 60 ppb.

A majority of NTOCs were measured at monitors surrounding the Ship Channel region. Figure 3.5 (left) compares the number of NTOCs recorded at each monitor from 2004-2008. Monitors are listed from left to right in order of increasing radial distance from the DRPK site. DRPK is co-located with numerous HRVOC point sources near the Ship Channel and observed the greatest number of NTOCs, 43, during the attainment

period. The shaded region of Figure 3.5 spans the 12 monitors that are within 20 km of DRPK. Though NTOCs were measured at every monitor, 70% were measured at the 12-monitor cluster indicating that NTOCs were not uniformly distributed.

## 3.2 Simulated Non-Typical Ozone Changes

The 8-h regulatory models developed by the TCEQ provide an opportunity to evaluate model performance with respect to high $O_3$ concentration gradients seen in measurements. Further, since HRVOC events were removed from the baseline emissions inventory, this provides an ideal scenario to test the model's sensitivity to day-specific emissions in the regulatory inventory.

The base case and baseline model runs both simulated NTOCs. Out of 120 episode days, there were a total of 664 simulated NTOCs in the base case; the baseline simulation predicted 431 NTOCs. Figure 3.2 shows the distribution of simulated $\Delta O_{3,1h}$ and subsequent 1-h concentrations for the base case (bottom left) and baseline (bottom right). Again, all data points above the top red line meet NTOC criterion 1. When compared to the 2004-2008 measurements (top right), two features stand out. First, the simulations were capable of reproducing the highest 1-h $O_3$ concentrations. Data points from the measurements, base case, and baseline all show maximum values above 180 ppb. The second feature is that neither simulation was able to reproduce the wide range of $\Delta O_{3,1h}$ present in the measurements. For example, the greatest predicted $\Delta O_{3,1h}$ was only 55 ppb/hr, which is only about half of the peak measurement, 106 ppb/hr. Figure 3.2 shows that the simulations are able to predict high concentrations via typical $O_3$ changes, but cannot replicate the highest $O_3$ resulting from NTOCs. It should also be mentioned that the base case and baseline distributions, while not identical, are similar.

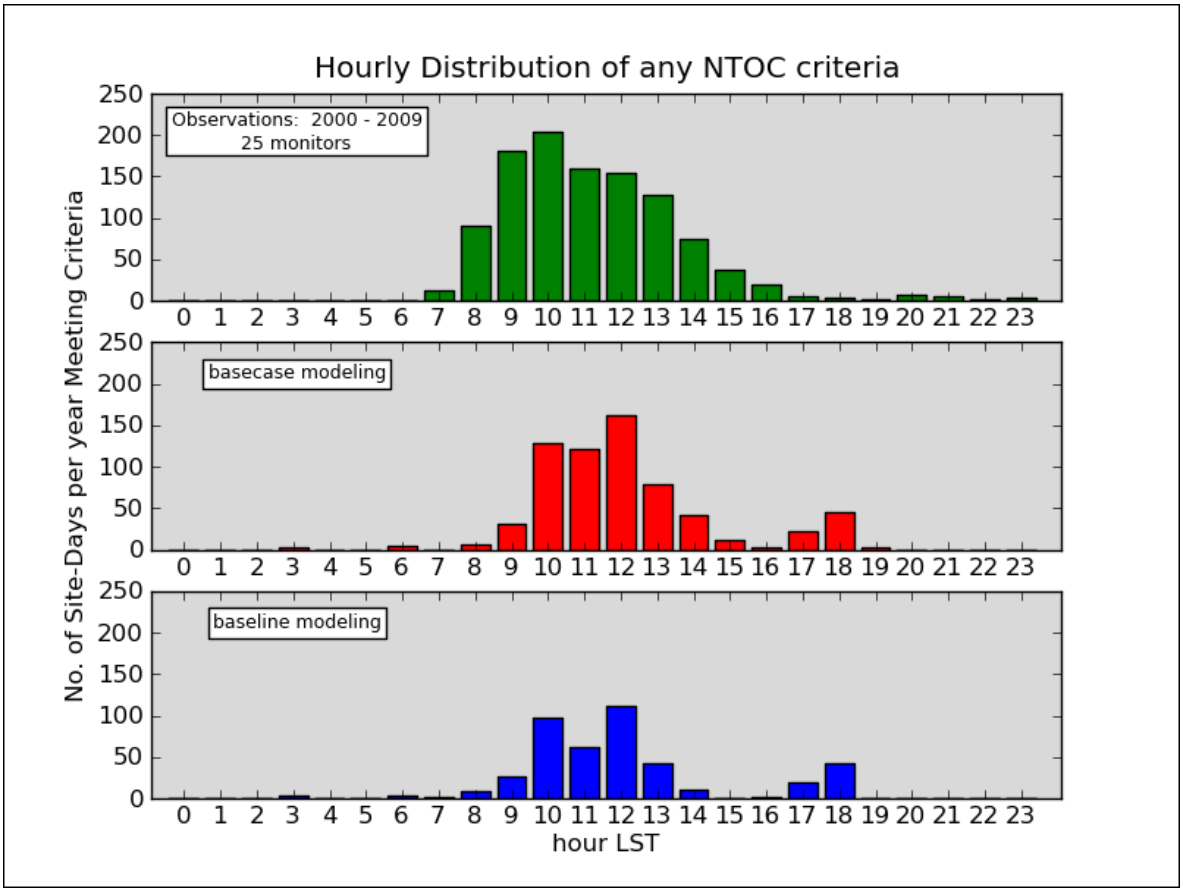


Figure 3.6: Temporal distribution of measured and simulated NTOCs. The plot on top shows all measured NTOCs from 2000-2009. The middle plot gives base case predicted NTOCs, and the bottom plot shows baseline predicted NTOCs. All episode days are included in the simulations shown in this figure.

Figure 3.5 (right) provides the spatial distribution of NTOCs simulated at the monitoring stations. Monitors are ordered by increasing distance from DRPK, and the shaded region encompasses those monitors within 20 km of DRPK. The data plotted represent only simulated NTOCs predicted within the 7x7 grid cell array centered on each monitor location; both the base case and baseline simulated NTOCs at grid cells elsewhere in the 2-km domain, but these are not represented in the figure. When only monitor-predicted NTOCs are considered, 74% of NTOCs were predicted within 20 km of DRPK, and this percentage increases to 79% for the baseline. These percentages are close to

the measured spatial distribution. Recall that 70% of NTOCs were measured within 20 km of the DRPK monitor.

Comparisons between the measured and simulated data shown in Figure 3.5 are limited and should be made carefully. The left hand plot spans a five-year period and provides only point measurements. The simulations, however, cover only 120 days, but are not limited to point measurements. They provide predictions for all locations within the modeled domain. Still, there are notable differences between the two plots. Base case and baseline simulations over predict the relative number of NTOCs at DRPK, HSMA, and HLAA. Simulated NTOCs at DRPK and HSMA are many times greater than at most other monitors within the shaded region, but measurements show less of a discrepancy between the Ship Channel monitors. Similarly, HLAA towers over most of the other monitors, but measurements show there were fewer NTOCs recorded there than almost anywhere else in Houston. SBFP and WALV show major under predictions in the relative number of simulated NTOCs. Measured NTOCs at SBFP and WALV were greater in number than nearly all other monitors, but almost none were predicted at those locations.

An examination of the simulated NTOC distribution in Figure 3.5 reveals differences between the base case and baseline. The base case almost always predicted more NTOCs at the monitors, and there were never more in the baseline. For example, there were 26 NTOCs predicted in the base case at HCQA, but none in the baseline. Only three NTOCs were simulated in the baseline at BAYP, down from 19 in the base case. DRPK, however, had the same number of NTOCs in the base case and baseline simulations. Overall, the monitors within the shaded region, i.e. near the Ship Channel region, had a 29% decrease in the number NTOCs when moving from the base case to the baseline. For the 13 monitors outside the shaded region, the percent decrease was much greater. Nearly half (48%) of simulated NTOCs that were present in the base case disappeared

in the baseline.

Temporal distributions of simulated (all episode days) and measured (2000-2009) NTOCs are shown in Figure 3.6. The base case predicted a maximum number of NTOCs at 1200 LST with about two-thirds happening between 1000 and 1300 LST. The baseline distribution has the same shape as the base case, but with attenuated totals for each hour. This matched relatively well with the observations, though there is a large discrepancy at hours 0800 and 0900 LST. Measurements show a large number of NTOCs occurred before 1000 LST, but neither the base case nor the baseline simulations matched those observations.

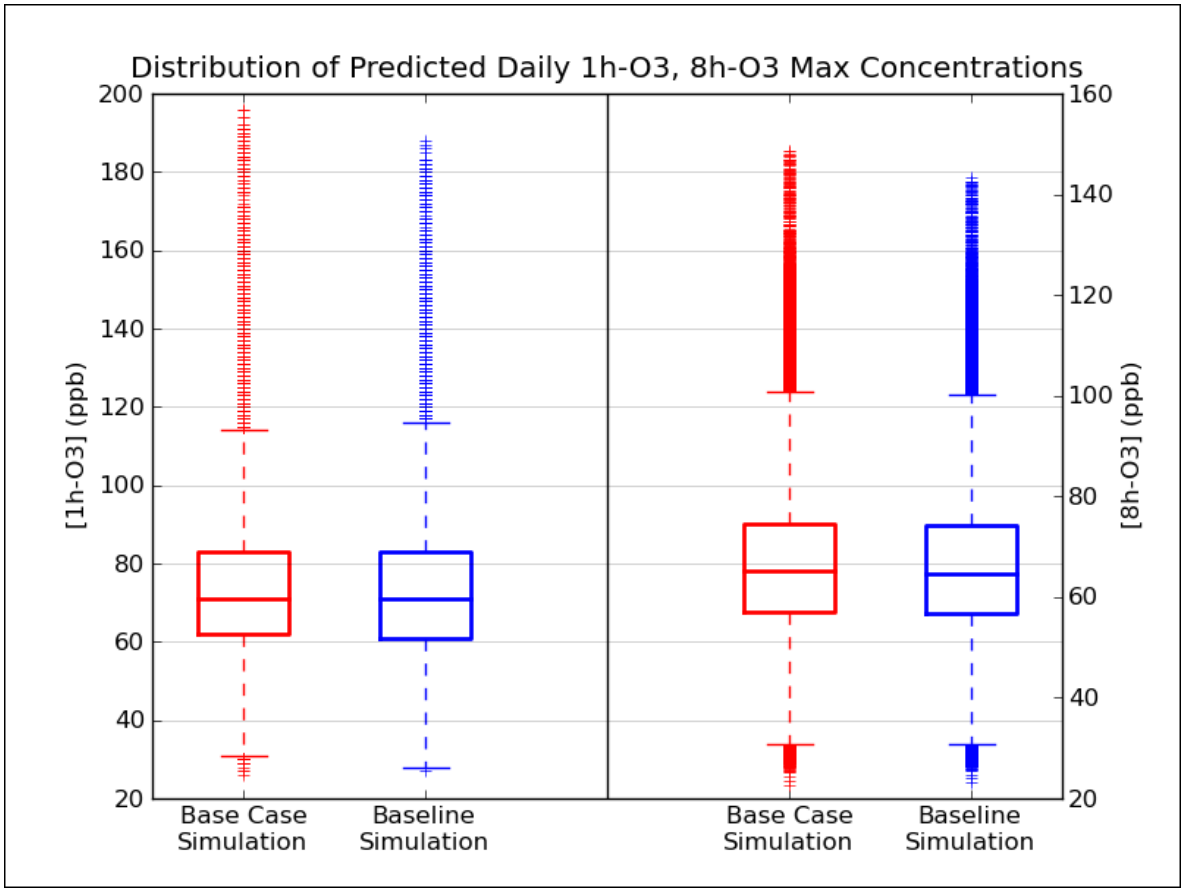


Figure 3.7: Distributions of 1-h and 8-h daily peak $O_3$ concentrations for all base case and baseline simulated episode days. The plot on the left gives 1-h maxima, and the plot on the right shows 8-h maxima.

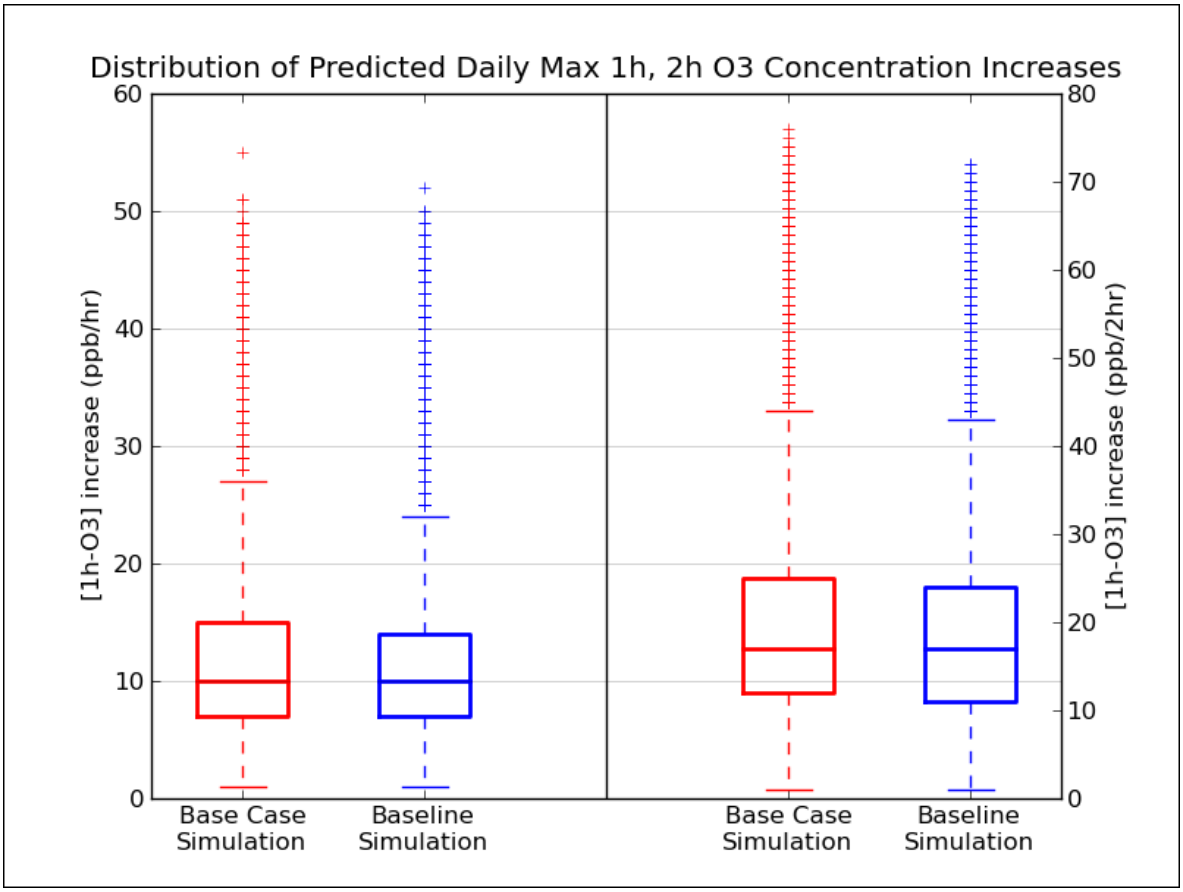


Figure 3.8: Distributions of daily maximum one-hour and two-hour $O_3$ concentration increases for all base case and baseline simulated episode days. The plot on the left gives maximum hourly increases, and the plot on the right shows maximum two-hour increases.

Seeing strong congruence between the base case and baseline model simulations in Figures 3.2 and 3.6, but marked differences in Figure 3.5, we made further comparisons between the two sets of predictions to better understand how the use of an averaged emissions inventory differs from the day-specific base case inventory. Distributions of peak 1-h and 8-h $O_3$ concentrations from the base case were compared alongside those same distributions from the baseline. These distributions are shown as box plots in Figure 3.7. There are remarkable similarities between the base case and baseline peak predictions. Median values are in perfect agreement, and the spread of data is nearly

identical. The base case simulation does predict slightly greater 1-h and 8-h maxima by 8 ppb and 6 ppb, respectively, which can only be explained by differences in the emissions inventories. Box plot distributions were also created for daily maximum $\Delta O_3$ from each grid cell. Given in Figure 3.8, peak rates of one-hour and two-hour increases show little difference between the base case and baseline. The base case, though, does predict marginally higher $\Delta O_3$ by a few parts per billion per hour.

## 3.3 Simulations of Observed Non-Typical Ozone Changes

Plumes with high spatial and temporal $O_3$ concentration gradients are measured several times each year in the Houston area. We have identified several plumes that met the NTOC criteria on days that were included in the TCEQ's regulatory modeling simulations. We then compared the measurements to baseline simulations to understand how well model predictions used in the attainment demonstration can reproduce extreme $O_3$ events.

One-hour $O_3$ time series measured at HLAA, BAYP, and HCQA are shown in Figure 3.9 (top) for September 7, 2006. HLAA is 15 km due north of BAYP, and HCQA is 8 km south of BAYP. Despite their proximity, $O_3$ concentrations and hourly changes are far greater at the BAYP monitor. Peak 1-h and 8-h values are 56 ppb and 24 ppb greater, respectively, than at either of the other nearby monitoring stations.

Model simulations were performed for September 7, 2006, and predicted baseline 1-h $O_3$ time series for HLAA, BAYP, and HCQA are given in Figure 3.9 (bottom). Comparisons to measurements show that the predictions failed to reproduce both the high 1-h $O_3$ values and the rapid rise in concentrations measured at BAYP. At 1100 LST, when the monitor encountered the leading edge of the ozone plume, measured 1-h $O_3$ was more than 20 ppb greater than predicted. That difference expanded to 41 ppb one hour later. The simulated maximum $\Delta O_{3,1h}$ was only 19 ppb/hr compared to a measured

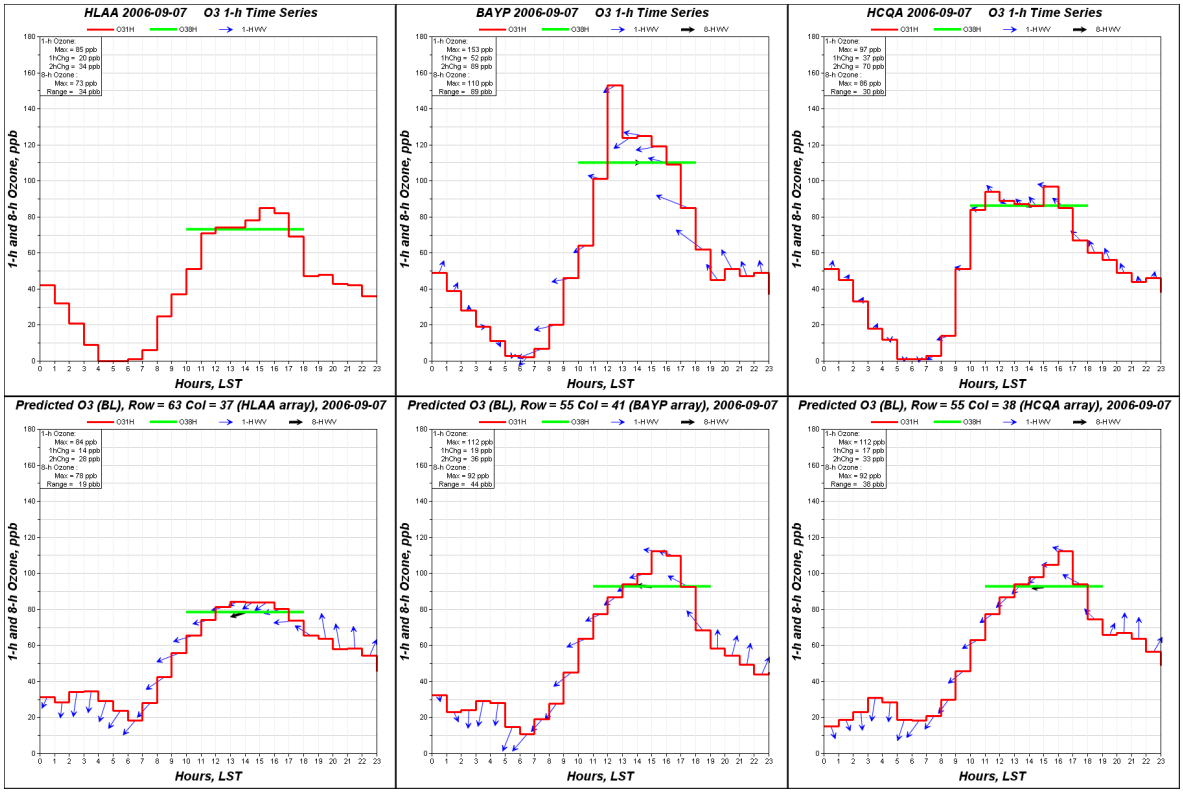


Figure 3.9: $O_3$ time series plots from measurements (top) and baseline simulations (bottom) for the HLAA, BAYP, and HCQA monitors on September 7, 2006. Hourly averaged $O_3$ concentrations are shown in red and hourly resultant wind vectors in blue. The green line represents the peak 8-h $O_3$ concentration, the 8-h window that was used, and a black arrow shows the 8-h resultant wind vector. Wind parameters are not measured at HLAA.

concentration increase of 52 ppb/hr. The maximum simulated 8-h $O_3$ concentration was 18 ppb lower than measured at the monitoring station as a consequence of the under predictions present in the model. Despite measured differences at BAYP and HCQA, simulated $O_3$ time series for the two monitors are almost identical, which led to under predictions at the former and over predictions at the latter. This indicates that, in the model, the monitors were likely affected by the same source. Measurements show that this was not true. Figure 3.10 shows predicted $O_3$ values mapped over the entire 2-km modeling domain for hours 1100-1400 LST. Diamonds mark the location

of ground monitoring stations, and the color of each diamond gives the measured $O_3$ concentration for a given hour. When a mismatch exists between grid cell color and diamond color, the model has either over or under predicted. Circles mark the monitors with the highest recorded $O_3$ concentrations at that hour, and there is a clear east to west progression of high $O_3$ measurements. The circled monitors also show severe model under predictions indicating that the simulations misplaced the highest $O_3$ .

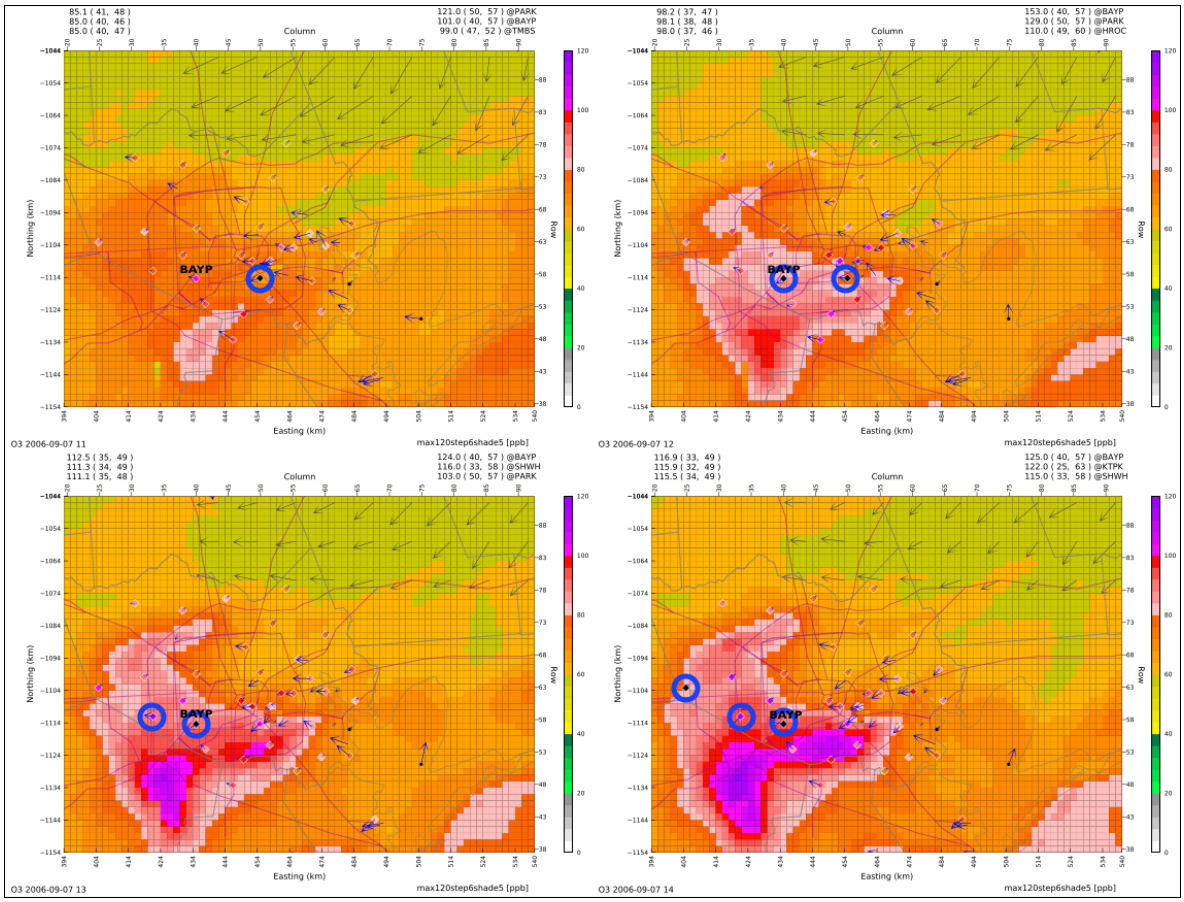


Figure 3.10: Baseline simulated spatial plots of 1-h $O_3$ concentrations for September 7, 2006 at 1100-1400 LST across the 2-km modeling domain. Diamond markers show the location of ground monitoring stations. The color of each diamond gives the measured 1-h $O_3$ value at that site. Black arrows at each diamond show the measured 1-h resultant wind vector at that site. Simulated 1-h resultant wind vectors are also shown for select grid cells. Blue circles mark the east to west progression of the highest $O_3$ measurements. The BAYP monitor is labeled.

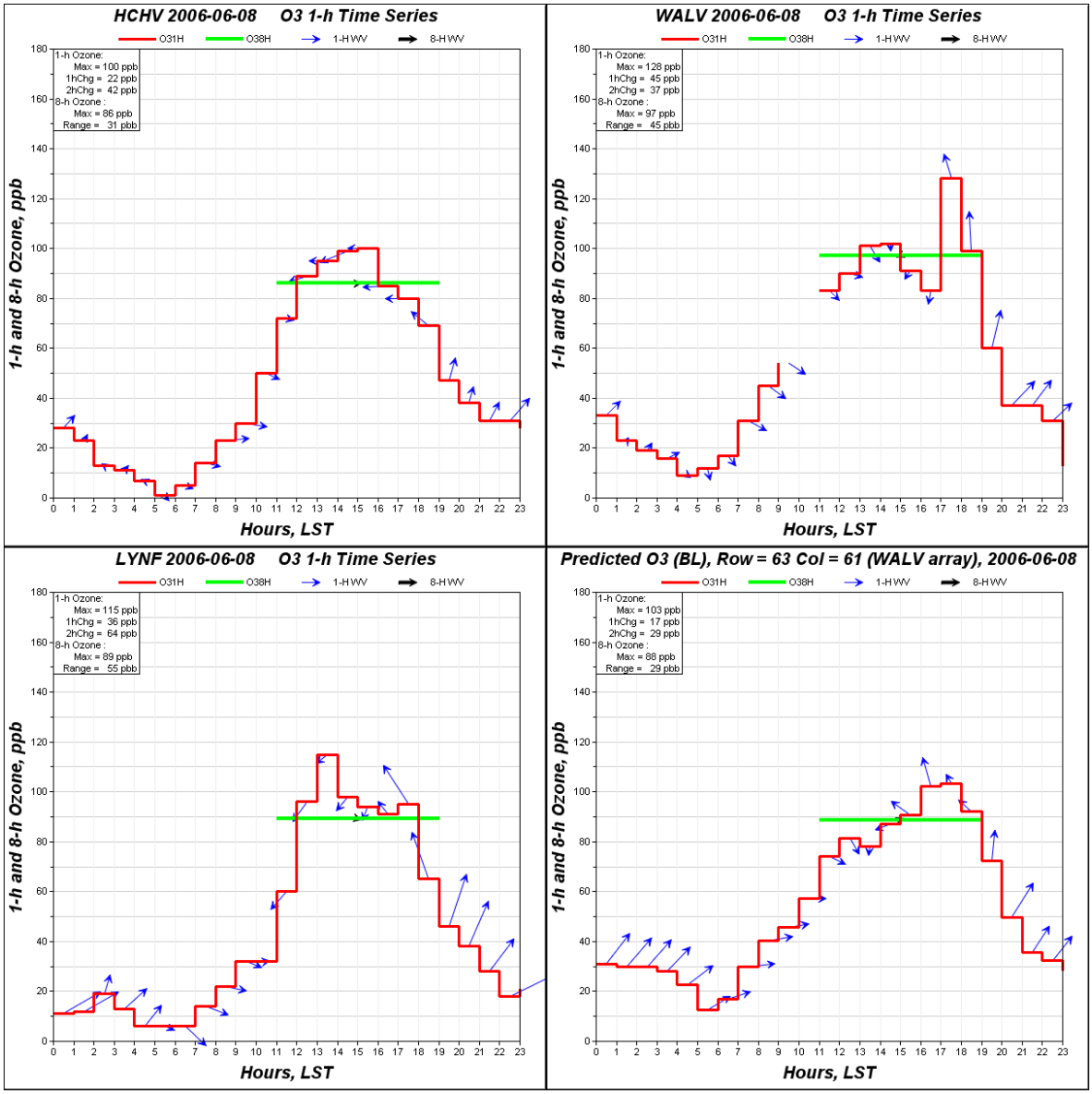


Figure 3.11: $O_3$ time series plots from measurements for the HCHV (top left), WALV (top right), and LYNF (bottom left) monitors on June 8, 2006. The bottom right plot shows simulated $O_3$ time series at WALV for the baseline simulation. Hourly averaged $O_3$ concentrations are shown in red and hourly resultant wind vectors in blue. The green line represents the peak 8-h $O_3$ concentration, the 8-h window that was used, and a black arrow shows the 8-h resultant wind vector.

A similarly isolated $O_3$ plume was measured at WALV on June 8, 2006. Figure 3.11 shows 1-h time series plots for WALV (top right) and two nearby monitors, HCHV (top

left) and LYNF (bottom left). At 1700 LST, WALV recorded a 45 ppb one-hour increase, which elevated peak $O_3$ to 128 ppb. Two hours later, the measured concentration fell to 60 ppb. The transient $O_3$ event was not recorded at HCHV or LYNF, both of which are located only about 10 km west of WALV. The baseline model simulation for WALV, displayed in Figure 3.11 (bottom right), does not include the observed late-afternoon $O_3$ spike, and, as a result, under predicted both 1-h and 8-h peak values. It is apparent from the WALV measurements that the late afternoon $O_3$ plume was transported from the south; wind direction reverses at 1700 LST, the exact hour that the 45 ppb/hr increase was measured. The baseline simulation predicts this wind reversal, and simulated $O_3$ concentrations increase to a maximum when winds shift to the north. But the magnitude of the increase is almost 30 ppb/hr less than measured.

Model simulations appear to have performed much better on August 17, 2006. Figure 3.12 shows measurements and predictions at DRPK on a day when rapidly increasing $O_3$ was observed. The model predicts the sudden concentration rise at 1100 LST to within 4 ppb/hr, and 1-h and 8-h maximum values more closely match measurements than the simulations shown in Figures 3.9 and 3.11. Time series plots (Figure 3.12, top left and bottom left) for monitors surrounding DRPK show that the high $O_3$ was not widespread in the measurements. Baseline simulation spatial plots are given in Figure 3.13 for hours 1100-1400 LST. High $O_3$ predictions blanket much of the region, and concentrations at nearly every monitor in south Houston were over predicted.

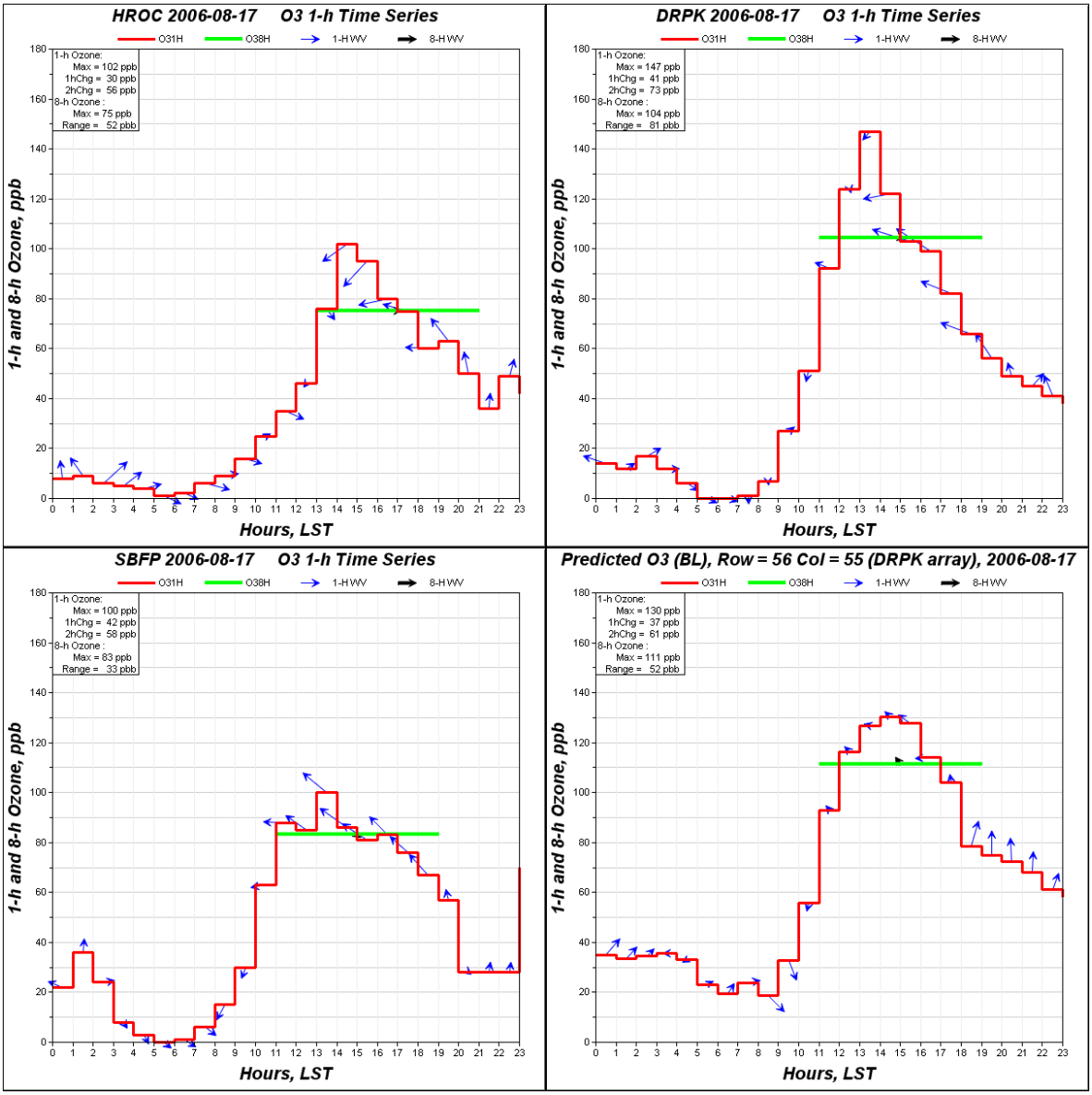


Figure 3.12: $O_3$ time series plots from measurements for the HROC (top left), DRPK (top right), and SBFP (bottom left) monitors on August 17, 2006. The bottom right plot shows simulated $O_3$ time series at DRPK for the baseline simulation. Hourly averaged $O_3$ concentrations are shown in red and hourly resultant wind vectors in blue. The green line represents the peak 8-h $O_3$ concentration, the 8-h window that was used, and a black arrow shows the 8-h resultant wind vector.

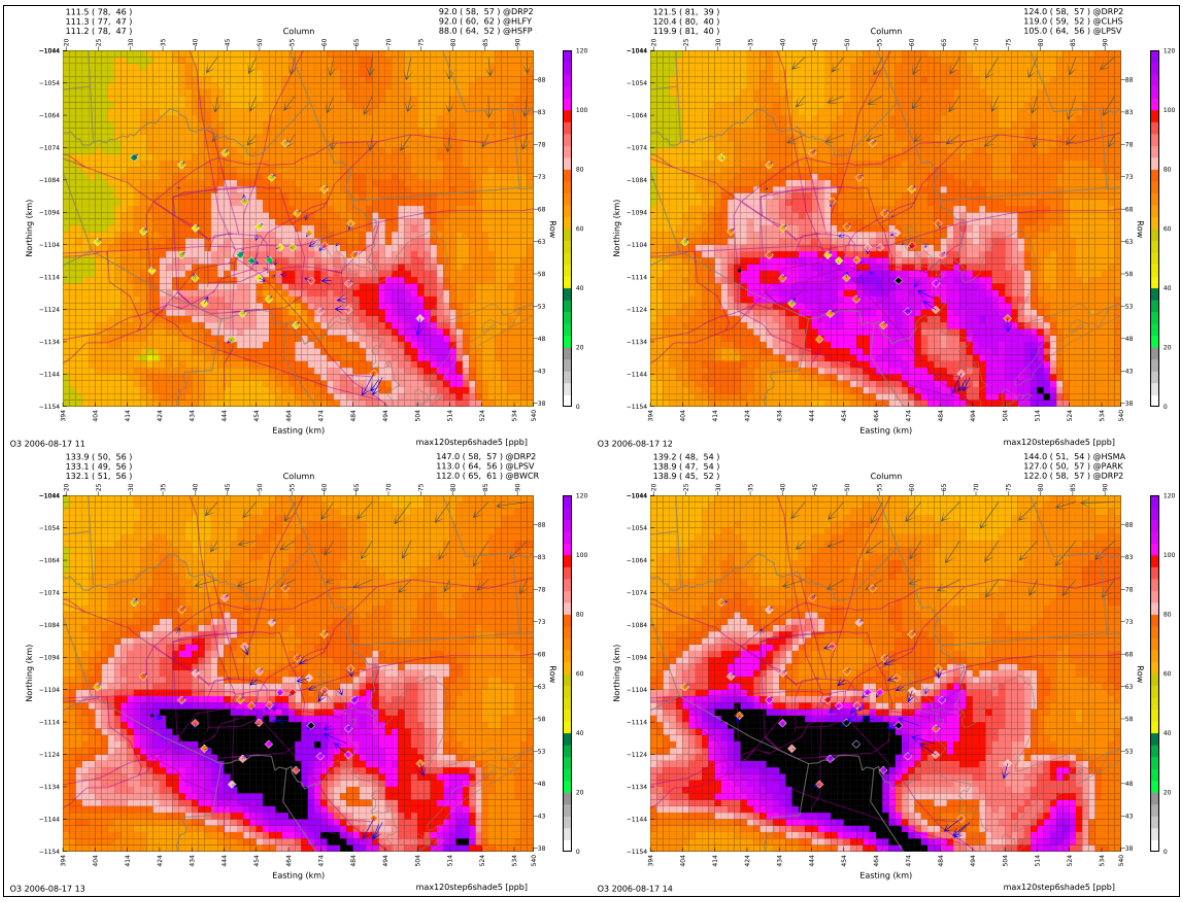


Figure 3.13: Baseline simulated spatial plots of 1-h $O_3$ concentrations for August 17, 2006 at 1100-1400 LST across the 2-km modeling domain. Diamond markers show the location of ground monitoring stations. The color of each diamond gives the measured 1-h $O_3$ value at that site. Black arrows at each diamond show the measured 1-h resultant wind vector at that site. Simulated 1-h resultant wind vectors are also shown for select grid cells.

# Chapter 4

# Discussion

This study investigated how non-typical ozone changes are represented in the 8-h NAAQS attainment methodology. High $O_3$ events and rapid $\Delta O_3$ are measured in Houston with considerable frequency, and the likelihood of an 8-h exceedance increases substantially on NTOC days. Twenty-five percent of all measured exceedances met one or both of the NTOC criteria from 2004-2008.

The current attainment methodology does not recognize the dual-$O_3$ formation paradigm that was used to develop the TCEQ's 2004 1-h $O_3$ SIP for Houston. Using a "typical" emissions inventory in regulatory modeling and averaging five years of observational data does not take into consideration the effects of stochastic HRVOC emissions events and high $\Delta O_3$ that disproportionately affect the most polluted days in Houston. We have quantified the effect measured NTOCs have on attainment demonstration outcomes.

The form of the 8-h $O_3$ NAAQS dictates that only annual $4^{th}$ highest daily maximum 8-h averages are used for assessing compliance with the federal standard. We considered all of the *four* highest 8-h $O_3$ days at each monitor, however, because the top three days necessarily influence which day has the $4^{th}$ highest concentration. Having identified the high-ozone days that influence the $DVb_i$ for a monitor (i.e. the four days with the highest daily maximum 8-h $O_3$ each year), the next step is to filter the data set to remove the

Table 4.1: List of monitoring stations and abbreviations with future attainment test results. $RRF_i$, $DVb_{i,2006}$, and $DVf_{i,2018}$ were calculated using the EPA attainment methodology. $DVb_{i,2006,filtered}$ is the 2006 baseline design value with all NTOC days removed from the data set, and $DVb_{i,2006}$ difference is the amount by which the $DVb_{i,2006}$ decreases after removing NTOC days. $DVf_i(DVb_{i,2006,filtered})$ is the recalculated final design value using $DVb_{i,2006,filtered}$ and $RRF_i$. $DVf_i$ difference is the amount by which the $DVf_i$ decreases when using $DVb_{i,2006,filtered}$ instead of $DVb_{i,2006}$.

| Monitor Name | Abbreviation | $RRF_i$ | $DVb_{i,2006}$ (ppb) | $Dvf_i$ (ppb) | $DVb_{i,2006,filtered}$ (ppb) | $DVb_{i,2006}$ difference (ppb) | $Dvf_i$ ($DVb_{i,2006,filtered}$) (ppb) | $Dvf_i$ difference (ppb) |
|---|---|---|---|---|---|---|---|---|
| Wallisville | WALV | 0.960 | 92.0 | 88.3 | 85.0 | -7.0 | 81.6 | -6.7 |
| Deer Park | DRPK | 0.958 | 92.0 | 88.1 | 82.0 | -10.0 | 78.6 | -9.6 |
| Bayland Park | BAYP | 0.899 | 96.7 | 86.9 | 93.7 | -3.0 | 84.2 | -2.7 |
| Monroe | HSMA | 0.934 | 90.3 | 84.3 | 82.0 | -8.3 | 76.6 | -7.8 |
| Manvel Croix Park | MACP | 0.900 | 90.7 | 81.6 | 87.7 | -3.0 | 78.9 | -2.7 |
| HRM-3 Haden Road | H03H | 0.959 | 84.0 | 80.6 | 82.3 | -1.7 | 78.9 | -1.6 |
| Texas City | TXCT | 0.947 | 84.3 | 79.8 | 82.3 | -2.0 | 77.9 | -1.9 |
| Seabrook Friendship Park | SBFP | 0.945 | 84.3 | 79.7 | 81.0 | -3.3 | 76.5 | -3.1 |
| Channelview | HCHV | 0.958 | 82.7 | 79.2 | 80.7 | -2.0 | 77.3 | -1.9 |
| Westhollow | SHWH | 0.858 | 92.3 | 79.2 | 92.0 | -0.3 | 78.9 | -0.3 |
| Aldine | HALC | 0.924 | 85.0 | 78.5 | 84.0 | -1.0 | 77.6 | -0.9 |
| Lynchburg Ferry | LYNF | 0.961 | 81.7 | 78.5 | 77.7 | -4.0 | 74.7 | -3.8 |
| Croquet | HCQA | 0.899 | 87.0 | 78.2 | 85.3 | -1.7 | 76.7 | -1.5 |
| Galveston | GALC | 0.955 | 81.7 | 78.0 | 81.7 | 0.0 | 78.0 | 0.0 |
| Northwest Harris County | HNWA | 0.873 | 89.0 | 77.7 | 89.0 | 0.0 | 77.7 | 0.0 |
| Mustang Bayou | MSTG | 0.917 | 84.7 | 77.7 | 84.7 | 0.0 | 77.7 | 0.0 |
| Houston East | HOEA | 0.958 | 80.3 | 76.9 | 79.3 | -1.0 | 76.0 | -1.0 |
| Houston Regional Office | HROC | 0.960 | 79.7 | 76.5 | 77.3 | -2.4 | 74.2 | -2.3 |
| Clinton | CLIN | 0.959 | 79.0 | 75.8 | 76.0 | -3.0 | 72.9 | -2.9 |
| Texas Avenue | HTCA | 0.941 | 79.3 | 74.6 | 78.0 | -1.3 | 73.4 | -1.2 |
| Conroe Relocated | CNR2 | 0.882 | 83.0 | 73.2 | 83.0 | 0.0 | 73.2 | 0.0 |
| Danciger | DNCG | 0.894 | 80.3 | 71.8 | 80.3 | 0.0 | 71.8 | 0.0 |
| North Wayside | HWAA | 0.938 | 76.3 | 71.6 | 75.7 | -0.6 | 71.0 | -0.6 |
| Lake Jackson | LKJK | 0.902 | 77.0 | 69.5 | 76.7 | -0.3 | 69.2 | -0.3 |
| Lang | HLAA | 0.891 | 77.7 | 69.2 | 77.3 | -0.4 | 68.9 | -0.4 |

NTOC days. The filtered data set is identical to the original data set except that all NTOC days have been removed. The $4^{th}$ highest day of this filtered set at each monitor becomes a part of a new filtered $DV_i$ calculation and is entered into the calculation of a filtered baseline design value, $DVb_{i,filtered}$. Filtered baseline design values for 2006 were calculated for all 25 monitors and are given in Table 4.1. $DVb_{i,2006}$ and $DVb_{i,2006,filtered}$ were then compared to quantify the effect of NTOCs on baseline design values.

Table 4.1 shows all the information relevant to the attainment demonstration for each monitor. $RRF_i$, $DVb_{i,2006}$, and $DVf_i$ were all calculated by following the EPA's recommended methodology. These results show that Houston has not demonstrated future attainment because WALV, DRPK, and BAYP all have $DVf_i$ above the federal standard. If

$DVb_{i,2006,filtered}$ are used in place of $DVb_{i,2006}$, however, every monitor passes the attainment test. At DRPK, the monitor that measured the greatest number of NTOCs, the baseline design value decreases by 10 ppb when NTOC days are removed from the calculation. This translated into a 9.6 ppb decrease in the $DVf_i$ when multiplied by the $RRF_i$. Similar decreases were seen at HSMA and WALV, two other monitors that are influenced by NTOCs.

Though NTOC behavior often leads to high $O_3$, Figure 3.2 shows that high peak $O_3$ can occur via typical concentration changes. The EPA attainment methodology discounts variable emissions as the leading determinant of peak $O_3$ leaving differences in day-to-day meteorology as the most important factor. Meteorology could be an explanation of NTOCs because high $\Delta O_3$ is sometimes observed without evidence of an HRVOC emissions event. Furthermore, meteorology is a known cause of high $O_3$ [26]. Uneven daytime heating of the land and sea (Galveston Bay) can create rotational winds that transport $O_3$ precursors offshore in the morning. Later in the day, the winds change direction and move the photochemically aged pollutants back across Houston. High $O_3$ concentrations and $\Delta O_3$ can result. The temporal distribution shown in Figure 3.6 indicates that, in fact, NTOCs often occur in the afternoon. There are also numerous NTOCs that are measured before 1000 LST. It is unlikely that Houston's rotational winds are the cause of these early morning NTOCs because there is not sufficient time for the rotational pattern to form. Whatever factors are causing the early NTOCs appear to be missing from the model simulations. Base case and baseline simulations under predict the number of NTOCs at 0800 and 0900 LST relative to other hours. Emissions events provide a permissible explanation for the early morning NTOCs in measurements. If fresh $NO_x$ from morning rush hour were to encounter a highly concentrated HRVOC plume, high $P(O_3)$ can be expected. The emissions event hypothesis can also explain the absence of NTOCs in the baseline simulations at 0800 and 0900 LST because the

baseline emissions inventory is void of such events.

Explaining the missing NTOCs in the base case is more problematic, however. The base case inventory is supposed to have day-specific emissions, but the simulations failed to create NTOCs in the early morning to the extent that was measured. This could mean that the emissions inventory missed, underestimated, or misplaced HRVOC sources. The hourly SI used in the base case was built from a combination of measurements and estimates of highly stochastic emissions point sources. Considering the large number of emissions upsets that occur in Houston each year, it is plausible that emissions rates reported in the SI are inaccurate. This would also help explain the similarities between the base case and baseline simulations. If HRVOC emissions in the base case inventory are not sufficient to simulate the maximum hourly $O_3$ concentrations and rates of change, removing them from the baseline emissions inventory might not make a noticeable difference.

Grid cell resolution is another possible explanation, and it has been shown to affect peak $O_3$ concentrations [27]. Point source emissions are instantaneously diluted into the entire grid cell volume. The TCEQ used 2-km grid cells in their regulatory modeling, which is a relatively fine resolution. If the dilution effect were great enough, however, it would explain the differences between base case predictions and measurements as well as the similarities between the base case and baseline simulations. A modeled emissions event would become too diluted to reach HRVOC concentrations necessary for high $P(O_3)$. Base case simulations running with diluted emissions would fail to match measurements and look similar to baseline predictions.

The reason for the under prediction at WALV (i.e. missing late afternoon peak) may signal missing HRVOC sources in the simulated environment or it could have been due to grid cell dilution. From Figure 3.11, it is apparent that the late afternoon $O_3$ plume was transported from the south; wind direction reverses at the exact hour when the

NTOC was measured. Base case and baseline simulations predict the wind reversal, but neither model run predicts the measured NTOC . Considering that the wind fields were correctly predicted, it is possible that the NTOC measured at WALV was induced by an emissions event that is missing from the emissions inventories. Alternatively, the event may have been included but was sufficiently diluted so as to remove the effects of the added emissions.

# Chapter 5

# Conclusions

Understanding how NTOCs are formed in the model has direct implications for the 8-h attainment demonstration. NTOCs are more likely to occur on high $O_3$ days in measurements and the model. Thus, discovering precursor reduction strategies that control NTOCs in the model will help reduce the highest simulated $O_3$ values. The effect on $DVb_{i,2006}$ alone can determine whether a particular monitor has passed the future attainment test. Our analysis here has brought the TCEQ's 1-h $O_3$ SIP conceptual model in line with the new 8-h attainment methodology.

Regulatory air quality models are able to simulate NTOC behavior, though not to the extent that it is observed. Higher $\Delta O_3$ values, which often lead to higher 1-h and 8-h $O_3$ concentrations, were found in the measurements than in either base case or baseline simulations. In general, base case and baseline simulations were very similar. They had identical median peak 1-h and 8-h $O_3$ values and comparable distributions of $\Delta O_{3,1h}$ and $\Delta O_{3,2h}$. Base case predictions usually predicted slightly greater maximum 1-h concentrations, possibly as a result of a more variable emissions inventory. Model simulations were unable to reproduce measured $\Delta O_3$ on many observed NTOC days. It is imperative for model simulations to accurately replicate this behavior because pollution control strategies are developed partly based on model response. If baseline simulations cannot match the high $\Delta O_3$ measured in the environment, it cannot be

reasonably assumed that future controls will limit their occurrence.

Two major questions remain that should be addressed in future work. First, it is not understood how the baseline simulation – without day-specific emissions – is able to simulate NTOCs. Process analysis can be utilized to understand the physical and chemical components of $O_3$ formation, and the processes at work in the baseline simulation can be compared to those in the base case. A more thorough analysis of the differences between the two emissions inventories may also assist in explaining how the baseline simulation is able to create NTOCs. The days with measured NTOCs that were analyzed in this study are good candidates for process analysis. Second, it has not been demonstrated that any NTOCs since 2003 have been caused by an HRVOC emissions event. Automated gas chromatograph data should be utilized to help identify possible HRVOC emissions events. When a likely event is discovered, a trajectory analysis can be conducted to ensure the suitability of meteorological parameters.

# Bibliography


[1] Texas Commission on Environmental Quality. Revisions to the State Implementation Plan (SIP) for the control of ozone pollution, 2004.

[2] H.E. Jeffries, S. Arunachalam, B.-U. Kim, D. Jobes, E. Pennington, A. Eyth, Z. Adelman, A. Holland, P. Pai, P. Partheepan, B. Schwede, and J. Vukovich. HARC Project H12.8HRB (UNC): Role of modeling assumptions in the Houston mid-course review; Final report to the Houston Advanced Research Center. Technical report, The University of North Carolina at Chapel Hill, Chapel Hill, NC, 2005.

[3] D. Allen, C. Murphy, Y. Kimura, W. Vizuete, T. Edgar, H.E. Jeffries, B.-U. Kim, M. Webster, and M. Symons. Texas Environmental Research Consortium Project H13: Variable industrial VOC emissions and their impact on ozone formation in the Houston Galveston area; Final report to the Texas Environmental Research Consortium. Technical report, The University of Texas at Austin and The University of North Carolina at Chapel Hill, Austin, TX and Chapel Hill, NC, 2004.

[4] L.I. Kleinman, P.H. Daum, D. Imre, Y.-N. Lee, L.J. Nunnermacker, and S.R. Springston. Ozone production rate and hydrocarbon reactivity in 5 urban areas: A cause of ozone concentration in Houston. *Geophys. Res. Lett.*, 29(10):1467–1470, 2002.

[5] P.H. Daum, L.I. Kleinman, S.R. Springston, L.J. Nunnermacker, Y.-N. Lee, J. Weinstein-Lloyd, J. Zheng, and C.M. Berkowitz. A comparative study of $O_3$ formation in the Houston urban and industrial plumes during the 2000 Texas Air Quality Study. *J. Geophys. Res.*, 108(D23):4715–4732, 2003.

[6] T.B. Ryerson, M. Trainer, W.M. Angevine, C.A. Brock, R.W. Dissly, F.C. Fehsenfeld, G.J. Frost, P.D. Goldan, J.S. Holloway, G. Hubler, R.O. Jakoubek, W.C. Kuster, J.A. Neuman, D.K. Nicks Jr., D.D. Parrish, J.M. Roberts, and D.T. Sueper. Effect of petrochemical industrial emissions of reactive alkenes and $NO_x$ on trophospheric ozone formation in Houston, Texas. *J. Geophys. Res.*, 108(D8):4249–4272, 2003.

[7] B.P. Wert, M. Trainer, A. Fried, T.B. Ryerson, B. Henry, W. Potter, W.M. Angevine, E. Atlas, S.G. Donnelly, F.C. Fehsenfeld, G.J. Frost, P.D. Goldan, A. Hansel, J.S. Holloway, G. Hubler, W.C. Kuster, D.K. Nicks Jr., J.A. Neuman, D.D. Parrish, S. Schauffler, J. Stutz, D.T. Seuper, C. Wiedinmyer, and A. Wisthaler. Signatures of terminal alkene oxidation in airborne formaldehyde measurements during TexAQS 2000. *J. Geophys. Res.*, 108(D3):4104–4117, 2003.

[8] C.F. Murphy and D.T. Allen. Hydrocarbon emissions from industrial release events in the Houston-Galveston area and their impact on ozone formation. *Atmos. Environ.*, 39(21):3785–3798, 2005.

[9] M. Estes. Update on TexAQS II findings. Southeast Texas Photochemical Modeling Committee meeting, June 20 2007.

[10] E. Cowling, C. Furiness, B. Dimitriades, and D. Parrish. Final rapid science synthesis report: Findings from the second Texas Air Quality study (TexAQS II); Final Report to the Texas Commission on Environmental Quality. Technical report, Southern Oxidants Study Office of the Director at North Carolina State University, Austin, TX, 2004.

[11] M. Webster, J. Nam, Y. Kimura, H.E. Jeffries, W. Vizuete, and D.T. Allen. The effect of variability in industrial emissions on ozone formation in Houston, Texas. *Atmos. Environ.*, 41(2007):9580–9593, 2007.

[12] W. Vizuete, B.-U. Kim, H.E. Jeffries, Y. Kimura, D.T. Allen, M.-A. Kioumourtzoglou, L. Biton, and B. Henderson. Modeling ozone formation from industrial emission events in Houston, Texas. *Atmos. Environ.*, 42(2008):7641–7650, 2008.

[13] P.H. Daum, L.I. Kleinman, S.R. Springston, L.J. Nunnermacker, Y.-N. Lee, J. Weinstein-Lloyd, J. Zheng, and C.M. Berkowitz. Origin and properties of plumes of high ozone observed during the Texas 2000 Air Quality Study (TexAQS 2000). *J. Geophys. Res.*, 109(D17306):doi:10.1029/2003JD004311, 2004.

[14] Y. Xie and C.M. Berkowitz. The use of positive matrix factorization with conditional probability functions in air quality studies: An application to hydrocarbon emissions in Houston, Texas. *Atmos. Environ.*, 40(2006):3070–3091, 2005.

[15] Texas Commission on Environmental Quality. Revision to the State Implementation Plan for the control of ozone air pollution: Houston-Galveston-Brazoria 1997 eight-hour standard nonattainment area, 2010.

[16] M. Estes. Overview of ozone exceedances in Houston and Dallas. Rapid Synthesis Briefing, TCEQ Air Modeling and Data Analysis Section, October 12 2006.

[17] U.S. Environmental Protection Agency. Guidance on the use of models and other analyses for demonstrating attainment of air quality goals for ozone, $PM_{2.5}$, and regional haze; EPA-454/B-07-002, 2007.

[18] W. Vizuete, H.E. Jeffries, T.W. Tesche, E.P. Olaguer, and E. Couzo. Issues with ozone attainment methodology for Houston, TX. *J. Air Waste Manag. Assoc.*, in press, 2010.

[19] Code of Federal Regulations. Interpretation of the 8-hour primary and secondary National Ambient Air Quality Standards for ozone, current through April 16, 2010.

[20] Texas Commission on Environmental Quality. Ozone Data. http://www.tceq.com/nav/data/ozone_data.html, last checked April 2010.

[21] ENVIRON International Corporation. *User's guide CAMx Comprehensive Air Quality Model with extensions*. Novato, CA, 2009.

[22] Texas Commission on Environmental Quality. Houston-Galveston-Brazoria Ozone Nonattianment Area. http://www.tceq.state.tx.us/implementation/air/sip/hgb.html, last checked April 2010.

[23] Texas Commission on Environmental Quality. Houston-Galveston-Brazoria 8-Hour Ozone SIP Modeling (2005/2006 Episodes): CAMx Modeling Domain. http://www.tceq.state.tx.us/implementation/air/airmod/data/hgb8h2/hgb8h2_camx_domain.html, last checked April 2010.

[24] W. Vizuete, L. Biton, H.E. Jeffries, and E. Couzo. Evaluation of relative response factor methodology for demonstrating attainment of 8-hr ozone in Houston, TX. *J. Air Waste Manag. Assoc.*, 60:838–848, 2010.

[25] D.T. Allen and J. Price. Accelerated science evaluation of ozone formation in the Houston-Galveston area: Atmospheric Chemistry. Technical report, 2001. http://www.utexas.edu/research/ceer/texaqsarchive/accerlerated.htm.

[26] R.M. Banta, C.J. Senff, J. Nielsen-Gammon, L.S. Darby, T. Ryerson, J. Alvarez, S. Sandberg, E. Williams, and M. Trainer. A bad air day in Houston. *Bull. Am. Meteorol. Soc.*, 86(5):657–669, 2005.

[27] B. Henderson. The influence of model resolution on ozone from industrial VOC releases. Master's thesis, The University of North Carolina at Chapel Hill, 2008.